



HAL
open science

“ Enhanced ” magnetism and nuclear ordering of ^{169}Tm spins in TmPO_4

C. Fermon, J.F. Gregg, J.-F. Jacquinot, Y. Roinel, V. Bouffard, G. Fournier,
A. Abragam

► To cite this version:

C. Fermon, J.F. Gregg, J.-F. Jacquinot, Y. Roinel, V. Bouffard, et al.. “ Enhanced ” magnetism and nuclear ordering of ^{169}Tm spins in TmPO_4 . *Journal de Physique*, 1986, 47 (6), pp.1053-1075. 10.1051/jphys:019860047060105300 . jpa-00210282

HAL Id: jpa-00210282

<https://hal.science/jpa-00210282>

Submitted on 4 Feb 2008

HAL is a multi-disciplinary open access archive for the deposit and dissemination of scientific research documents, whether they are published or not. The documents may come from teaching and research institutions in France or abroad, or from public or private research centers.

L'archive ouverte pluridisciplinaire **HAL**, est destinée au dépôt et à la diffusion de documents scientifiques de niveau recherche, publiés ou non, émanant des établissements d'enseignement et de recherche français ou étrangers, des laboratoires publics ou privés.

Classification

Physics Abstracts

75.25 — 76.30K — 76.70E

« Enhanced » magnetism and nuclear ordering of ^{169}Tm spins in TmPO_4

C. Fermon, J. F. Gregg (*), J.-F. Jacquinot, Y. Roinel, V. Bouffard, G. Fournier and A. Abragam

Service de Physique du Solide et de Résonance Magnétique,
CEN-Saclay, 91191 Gif sur Yvette Cedex, France

(Reçu le 16 décembre 1985, révisé le 6 février 1986, accepté le 17 février 1986)

Résumé. — L'ordre des spins nucléaires de ^{169}Tm dans le TmPO_4 , produit par leur magnétisme « renforcé », a été créé par Polarisation Dynamique Nucléaire (D.N.P.) suivie par une Désaimantation Adiabatique dans le Référentiel Tournant (A.D.R.F.). A température positive, avec le champ magnétique \mathbf{H} orienté le long de l'axe c du cristal, la structure est transverse dans le référentiel tournant, donc apparaît comme tournant à la fréquence de Larmor dans le référentiel du laboratoire. Cet article décrit en détail : 1) L'influence de l'orientation de \mathbf{H} sur la largeur de raie R.M.N., et les procédés expérimentaux utilisés pour contrôler cette orientation et obtenir les meilleurs résultats en D.N.P. 2) La relaxation nucléaire des ^{169}Tm et des ^{31}P lorsque \mathbf{H} est presque parallèle à c . 3) Les mesures de R.M.N. sur le ^{169}Tm et les expériences de double résonance avec le ^{31}P qui confirment la nature de l'état ordonné et qui sont comparées aux prévisions théoriques (Weiss et R.P.A.).

Abstract. — Ordering of the nuclear spins of ^{169}Tm in TmPO_4 , caused by their « enhanced » nuclear magnetism, has been produced by Dynamic Nuclear Polarization (D.N.P.) followed by Adiabatic Demagnetization in the Rotating Frame (A.D.R.F.). At positive temperature, when the magnetic field \mathbf{H} is parallel to the c -axis of the crystal, the structure is transverse in the rotating frame, thus appearing as rotating at the Larmor frequency in the laboratory frame. This article describes in detail : 1) The influence of the orientation of \mathbf{H} on the N.M.R. linewidth, and the experimental procedures used to control this orientation and optimize the D.N.P. results. 2) The nuclear relaxation of ^{169}Tm and ^{31}P when \mathbf{H} is almost parallel to c . 3) The ^{169}Tm N.M.R. measurements and the double resonance experiments using ^{31}P which confirm the nature of the ordered state and are compared to the theoretical predictions (Weiss and R.P.A.).

1. Introduction.

Nuclear magnetic ordering has been studied in a number of diamagnetic crystals [1-8]. With the important exception of ^3He , the ordering temperature of these substances (determined by the dipolar interaction between nuclear spins) is in the microkelvin range, and the cooling of the nuclei is obtained by a two-step process : 1) Dynamic Nuclear Polarization (D.N.P.), which brings the nuclear spin temperature into the millikelvin range, and 2) Adiabatic Demagnetization in the Rotating Frame (A.D.R.F.), which lowers the spin temperature by a factor of 1 000, and leaves the sample in a high field where its ordered state can be studied by Nuclear Magnetic Resonance (N.M.R.).

The need for dynamic polarization is imposed by the extreme slowness of the nuclear relaxation at low

lattice temperature. This difficulty is generally absent in metals, where the nuclear relaxation obeys the Korringa law. In copper, the ordering temperature (of the order of 100 nanokelvin), has also been obtained by a two-step process [9], in which the precooling of the nuclei is produced by thermal contact with a very powerful refrigerator, and the demagnetization is performed in the « Laboratory Frame ».

There exists a third class of substances in which nuclear cooling and nuclear ordering have been observed [10-14], the so-called « Van Vleck compounds ». In the latter, the singlet electronic ground state of a non-Kramers lanthanide ion is magnetized by hyperfine interaction with the nuclear spin \mathbf{I} of the ion : there appears an electronic magnetic moment $\hbar\gamma_1 \mathbf{KI}$. Hence the total magnetic moment can be considered as due to a nucleus carrying an « enhanced » gyromagnetic factor $\gamma = \gamma_1(1 + \mathbf{K})$. The tensor \mathbf{K} is very anisotropic, and some of its principal values are much larger than unity, which has two consequences from the point of view of nuclear

(*) Permanent address : The Clarendon Laboratory, University of Oxford, Parks Road, Oxford OX1 3PU, U.K.

magnetic ordering :

1) The large anisotropy favours ordered structures in which the spins are quantized along the directions where γ is maximum.

2) The large gyromagnetic factor increases the transition temperature with respect to a crystal with purely nuclear magnetism (up to a few mK in some cases), and decreases the nuclear relaxation times so that « brute force » polarizations become feasible.

Indeed, in the experiments of ordering reported so far in Van Vleck compounds, the nuclear spins have been polarized, then demagnetized by « brute force ». The aim of this article is to describe some ordering experiments performed in thulium phosphate (TmPO_4), using the same techniques as for diamagnetic crystals. They include 1) An experimental study of the nuclear relaxation in TmPO_4 in high field at low temperature. 2) D.N.P. of the ^{169}Tm and ^{31}P nuclear spins (henceforth Tm and P respectively), and 3) Observation of a helical transverse ordered phase of Tm in the rotating frame, phase which is thus rotating in the laboratory frame. The technique used to observe this ordered state is N.M.R. in high field. We discuss also in this article some experimental procedures necessary to adapt the apparatus to the special requirements (due to anisotropy) of this type of compound. A preliminary report on these results has been published previously [15].

2. N.M.R. properties and D.N.P.

2.1 GENERAL CONSIDERATIONS. — The general methods used for the study of nuclear magnetism and nuclear magnetic ordering in high field have been reviewed in [7-8]. The theoretical background for the application of these studies to Van Vleck compounds is laid out in [16]. We summarize briefly below the relevant characteristics of TmPO_4 :

The Tm^{3+} ion has the structure $4f_{12}, 3H_6$. To a very good approximation, the low-lying energy level of the free ion is a multiplet $J = 6$ with the first excited multiplet $J = 5$ some 8400 cm^{-1} higher. TmPO_4 has the tetragonal zircon structure (Fig. 1), and the effect of the Tm^{3+} interaction with the crystal field created by the neighbouring ions partially lifts the $2J + 1$ degeneracy, leaving one non-Kramers singlet ground state with a low-lying doublet at about 29 cm^{-1} . For more details about the electronic structure in TmPO_4 , see for instance [17]. To first order, this singlet is non-magnetic. To second order, admixing of the first excited states under the influence of a magnetic field leads to the appearance of a magnetization. Two cases can be considered :

1) The magnetization induced by the external, homogeneous magnetic field \mathbf{H} :

$$\langle \mathbf{M}_H \rangle = (g_J \mu_B)^2 \mathfrak{C} \mathbf{H}. \quad (1)$$

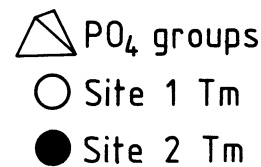
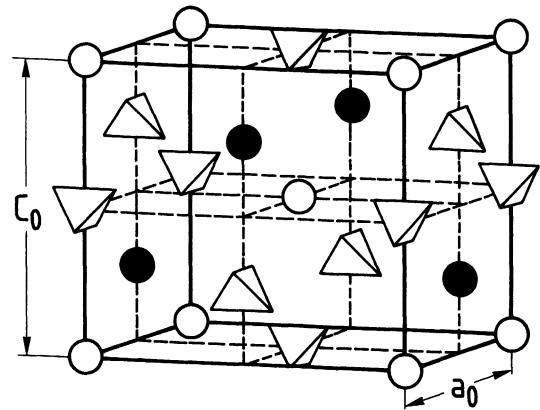


Fig. 1. — Crystalline structure of TmPO_4 , $a_0 = 6.847 \text{ \AA}$, $c_0 = 5.994 \text{ \AA}$.

This is the Van Vleck paramagnetism, which, unlike ordinary paramagnetism, is independent of temperature.

2) The magnetization induced by the hyperfine interaction with the nuclear spin \mathbf{I} of the thulium ion :

$$\langle \mathbf{M}_I \rangle = A_J g_J \mu_B \mathfrak{C} \langle \mathbf{I} \rangle. \quad (2)$$

This is the enhanced, or pseudo-nuclear magnetism.

In the above formulae, $g_J = 7/6$ is the Landé-factor inside the multiplet J , A_J is the hyperfine coupling constant with the nucleus, μ_B is the Bohr magneton, and the components of the tensor \mathfrak{C} are given [16] by :

$$\mathfrak{C}_{\alpha\beta} = \sum' \frac{\langle 0 | J_\alpha | n \rangle \langle n | J_\beta | 0 \rangle}{E_n - E_0}. \quad (3)$$

The tensor has axial symmetry, the anisotropy axis lying along the c -direction.

The fact that $\langle \mathbf{M}_H \rangle$ and $\langle \mathbf{M}_I \rangle$ are rigorously proportional, although they have quite different origins, is a consequence of the Wigner-Eckart theorem : J is a good quantum number in TmPO_4 , and inside the J -manifold the expectation value of all vectors are proportional.

Adding (2) to the nuclear magnetic moment gives for the pseudo-nuclear gyromagnetic tensor :

$$\gamma = \gamma_I \left[1 + \frac{A_J g_J \mu_B}{\hbar \gamma_I} \mathfrak{C} \right] \quad (4)$$

which has principal values :

$$\gamma_{\parallel}/2\pi = 11.33 \text{ MHz/tesla} \quad (5)$$

$$\gamma_{\perp}/2\pi = 274 \text{ MHz/tesla} \quad (6)$$

as compared to the « bare » nuclear value :

$$\gamma_1/2\pi = 3.5 \text{ MHz/tesla.} \quad (7)$$

Numerical values for the Van Vleck magnetization are :

$$\langle M_H \rangle_{\parallel} = 3.2 \text{ Gauss/tesla} \quad (8)$$

$$\langle M_H \rangle_{\perp} = 110 \text{ Gauss/tesla.} \quad (9)$$

Considering the effect of the anisotropic gyromagnetic tensor γ alone, it is shown in [16] that if a sample of TmPO₄ is subjected to a field H which makes an angle θ with the anisotropy axis (z-axis), and exposed to a radio-frequency field H_1 perpendicular to Oz, the motion of the spins can be described in the usual way using a frame OXYZ, with OX = Ox and OZ making an angle ϕ with the z-axis, such that :

$$\tan \phi = \gamma_{\perp}/\gamma_{\parallel} \tan \theta. \quad (10)$$

In this frame the Hamiltonian describing the motion of the spins becomes :

$$\mathcal{H} = \omega_0 I_z + 2\omega_1 I_x \cos \omega t \quad (11)$$

with

$$\omega_0 = \gamma H \quad \text{and} \quad \omega_1 = \gamma_{\perp} H_1 \quad (12)$$

where the effective gyromagnetic factor γ is given by :

$$\gamma = (\gamma_{\parallel}^2 \cos^2 \theta + \gamma_{\perp}^2 \sin^2 \theta)^{1/2}. \quad (13)$$

We examine now the effect of the above considerations on the N.M.R. linewidth. In the remainder of the article we will assume that θ is always very small, unless the contrary is explicitly stated. The case $\theta = \pi/2$ has been treated in a previous article [18].

2.2 N.M.R. LINEWIDTH. — The experimental variation of the N.M.R. linewidth of thulium at a constant frequency of 37 MHz as a function of the angle θ is plotted in figure 2b, where the sharp angular dependence is evident. In order to minimize the linewidth, it is necessary to orient the crystal with respect to the magnetic field with an accuracy better than a tenth of a degree. Since it was not possible with our apparatus to move the sample inside the dilution refrigerator, the sample was first oriented as accurately as possible using X-rays, the residual error being of the order of one degree. Then the magnetic field was aligned along the c-axis of the crystal using a set of compensating coils with axis perpendicular to the main field. The variation of θ in figure 2b was obtained as follows : the two compensating currents were first set to their optimum values, then the current in one coil was varied, while the other remained constant.

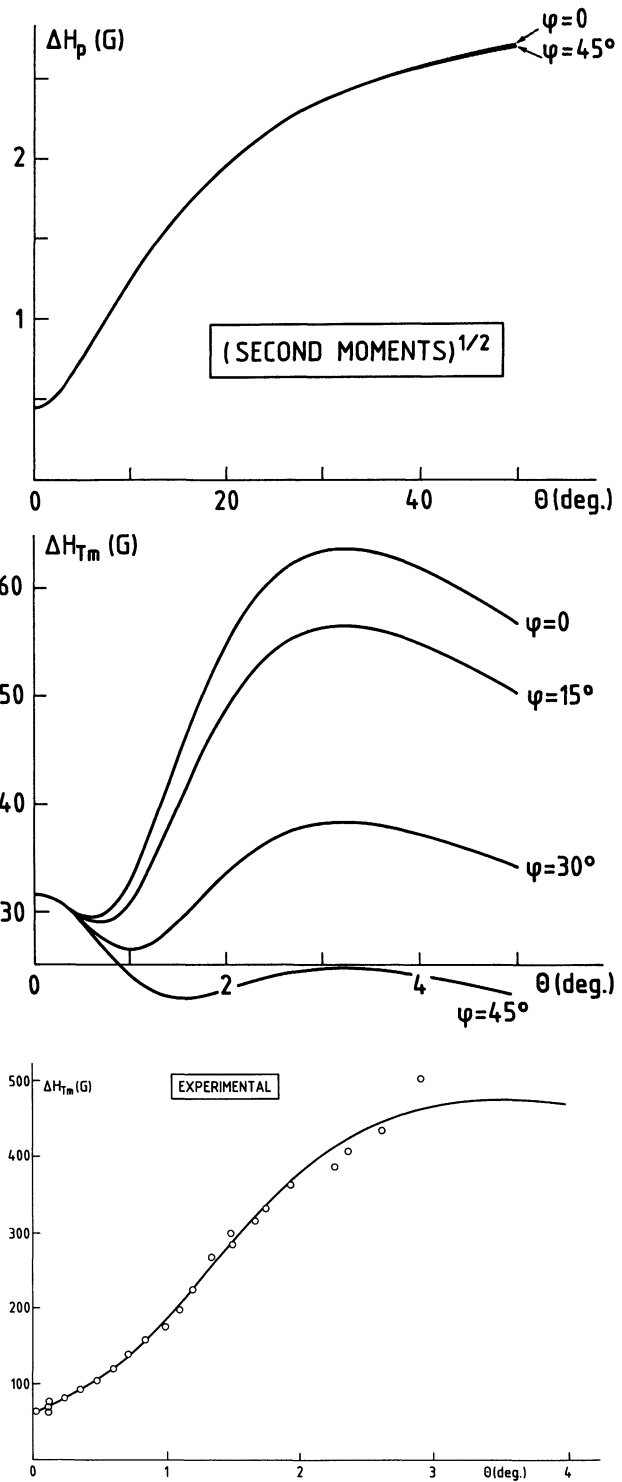


Fig. 2. — a) Square root of the theoretical second moment in Gauss for ³¹P (top) and for ¹⁶⁹Tm (bottom), at a fixed frequency of 37 MHz as a function of the polar angles θ and ϕ of the magnetic field with respect to the crystalline axes ($H_0 \parallel (100)$ corresponds to $\theta = \frac{\pi}{2}$ and $\phi = 0$). b) Experimental FWHM of the ¹⁶⁹Tm (open circles) and theoretical fit (full line).

When analysing the origin of the linewidth, several causes of broadening should be considered [19-20] :

2.2.1 *Intrinsic broadening.* — We consider only the dipolar coupling between the enhanced nuclear moments as given by equation (30) of reference [16]. Other intrinsic broadening mechanisms are negligible. The square root ΔH_{ss} of the second moment of the N.M.R. lines of Tm and P under the effect of the dipolar interactions is shown on figure 2a.

The effect of the intrinsic broadening would be an homogeneous linewidth, independent of magnetic field for a given orientation. For $\theta = 0$, this gives $\Delta H_{ss} = 32$ Gauss for Tm and 0.4 Gauss for P (Fig. 2a).

2.2.2 *Extrinsic causes of broadening.* — a) The inhomogeneity of the internal field : the magnetization (essentially the Van Vleck magnetization $\langle M_H \rangle$) of the Tm ions causes a strong internal field the amplitude of which is dependent upon the shape of the sample. When the sample is not an ellipsoid, this internal field is not homogeneous and causes a broadening of the lines. A typical internal field distribution in a rectangular sample of dimensions $2 \times 2 \times 4$ mm (magnetization, c -axis and field along the larger dimension) is shown in figure 3. The linewidth at half height in this example is of the order of $\langle M_H \rangle$, or ≈ 3 Gauss/tesla (the exact value depending on whether the sharp peak of figure 3 is broadened by dipolar interactions). Experimentally, we found :

P frequency	Field	Experimental width	$\langle M_H \rangle$
29 MHz	1.2 T	9 Gauss	5.5 Gauss
59 MHz	3.4 T	17 Gauss	11 Gauss

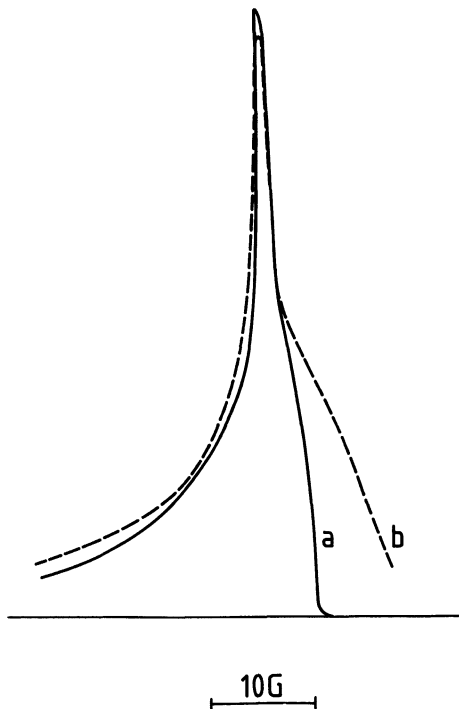


Fig. 3. — a) Theoretical distribution of internal field in a $2 \times 2 \times 4$ mm³ rectangular sample of TmPO₄, for $H_0 \parallel c$. b) Experimental linewidth of ³¹P.

Owing to the approximations made, the P linewidth is correctly described by the inhomogeneity of the internal field. For Tm, there are additional causes of extrinsic broadening [19-20] :

b) The crystalline mosaicity.

c) The random local strains, which cause fluctuations in the values of the tensor (by modulating the energy of the excited doublet) and a scatter in the angular distribution of the local crystalline axes, thereby contributing to the mosaicity.

Let $A = \gamma_{\perp}/\gamma_{\parallel}$ be the anisotropy factor, $\langle \delta\gamma_{\parallel}^2 \rangle/\gamma_{\parallel}^2$ and $\langle \delta\gamma_{\perp}^2 \rangle/\gamma_{\perp}^2$ the quadratic fluctuations of the principal values of the γ -tensor, and $\langle \delta\theta^2 \rangle$ the fluctuation of θ due to the mosaicity. The extra linewidth at constant frequency due to the above causes is given, for small values of θ by :

$$\Delta H_{sc} = H_0 \left[\frac{\langle \delta\gamma_{\parallel}^2 \rangle}{\gamma_{\parallel}^2} + A^2 \theta^2 \langle A^2 \delta\theta^2 \rangle + A^4 \theta^4 \frac{\langle \delta\gamma_{\perp}^2 \rangle}{\gamma_{\perp}^2} \right]^{1/2} (1 + A^2 \theta^2)^{-3/2} \quad (14)$$

where H_0 is the resonant field for $\theta = 0$.

d) The inhomogeneity of the static field. This last term was not considered in the previous works [19-20], since it is introduced by our compensating coils. It is equivalent to a mosaicity $\langle \delta\theta^2 \rangle$ proportional to the current in the compensating coils. If θ is the angle for zero compensating current, this « pseudo-mosaicity » is given by :

$$\langle \delta\theta^2 \rangle = \alpha' i^2 = \alpha(\theta - \theta_0)^2. \quad (15)$$

The extrinsic broadening is proportional to the magnetic field, and should disappear at sufficiently low frequency. However, it predominates for $\theta \neq 0$ under the conditions of our experiment. It is very difficult to separate out the different extrinsic effects. Nethertheless, it would seem that the inhomogeneity of the compensating field predominated over the true mosaicity : on the one hand, the data are impossible to fit accurately unless the former is taken into account ; on the other hand, we get a very reasonable fit of the experimental data by neglecting completely the latter. For that purpose, we replace $\langle \delta\theta^2 \rangle$ by $\alpha(\theta - \theta_0)^2$ in the expression (14). The *total* width ΔH is given by :

$$\Delta H = 2.1(\Delta H_{ss}^2 + \Delta H_{sc}^2)^{1/2} \quad (16)$$

with ΔH_{sc} of the form :

$$H_0 [a + b\theta^2(\theta - \theta_0)^2 + c\theta^4]^{1/2} (1 + A^2 \theta^2)^{-3/2}$$

in (16) the coefficient 2.1 between the full width at half maximum and the square root of the 2nd moment assumes a Gaussian lineshape. The fit yields values of

a , b and c from which we deduce :

$$\frac{\langle \delta\gamma_{\parallel}^2 \rangle^{1/2}}{\gamma_{\parallel}} \ll 2 \times 10^{-3}; \quad \frac{\langle \delta\gamma_{\perp}^2 \rangle^{1/2}}{\gamma_{\perp}} = 3.5 \times 10^{-2};$$

$$\frac{\langle \delta\theta'^2 \rangle^{1/2}}{\theta - \theta_0} = 2.7 \times 10^{-2}. \quad (17)$$

The last figure indicates that, for an initial misalignment of 1 deg., the compensating field scatters the angle by 2.7×10^{-2} deg., or 1.6 min. This result is in fair agreement with the transverse field inhomogeneity which can be computed from the shape and size of the compensating coils. It is a little surprising but still possible that the true mosaicity should be smaller than 1.6 min.

2.2.3 Reproducibility. — The above values varied somewhat from one sample to another and indeed, for a given sample, they varied from one experiment to the next, depending apparently on the thermal history of the sample. The samples seem to be rather sensitive to thermal cycling, and some were found to have cleaved after an experiment at low temperature. Other ones were not cleaved, but were broadened at $\theta = 0$ indicating an anomalously large $\langle \delta\gamma_{\parallel}^2 \rangle / \gamma_{\parallel}^2$. These crystals could be cured successfully by heating at 1 000 °C for 12 hours. We conclude this study by pointing out that, due to a variety of extrinsic causes, the N.M.R. line of Tm is inhomogeneously broadened, unless great care is taken, such as aligning carefully the magnetic field along the crystal. The consequences of this broadening for dynamic polarization will be examined in 2.4.

2.3 NUCLEAR RELAXATION.

2.3.1 Thermal mixing. — To explain the nuclear relaxation with H_0 parallel to c , it is necessary to take into account the effects of thermal mixing between Tm and P. The experiments were carried out in the following manner : the nuclear spin system was prepared out of equilibrium with the lattice, either by saturation, or by D.N.P. The combination of these techniques allowed the establishment of initial nuclear spin temperatures different from each other and from the lattice temperature. The subsequent recovery of both species was observed separately. In an « ideal » thermal mixing experiment [21] the spin-spin interactions of paramagnetic impurities present in the sample bring the various nuclear spin species rapidly to the same temperature, then the common spin temperature relaxes more slowly towards the lattice.

The situation here is slightly different. As an example, we show in figure 4 the evolution of the Tm and P spin temperatures at $T = 150$ mK and $H = 0.8$ tesla, with two different initial conditions :

In figure 4a, $P_{\text{Tm}} = 3.75\%$ ($T_{\text{Tm}} = 5.75$ mK),
 $P_{\text{P}} = 0$ ($T_{\text{P}} = \infty$).
 In figure 4b, $P_{\text{Tm}} = 0$ ($T_{\text{Tm}} = \infty$), $P_{\text{P}} = 7.1\%$
 ($T_{\text{P}} = 4.6$ mK).

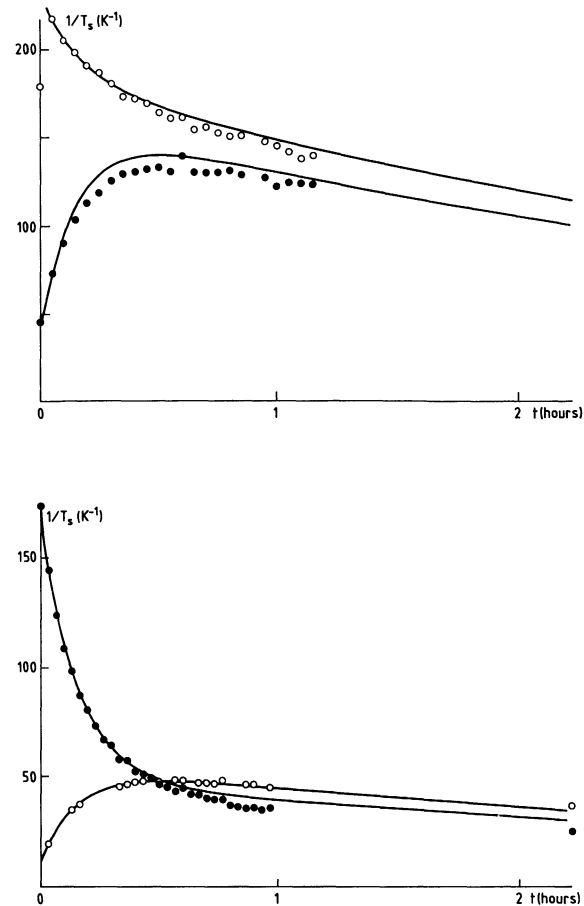


Fig. 4. — Relaxation in 0.8 tesla of the ^{169}Tm (open circles) and ^{31}P (closed circles) inverse spin temperatures $1/T_s$, for different initial conditions; a) $P(\text{Tm}) = 3.75\%$; $P(\text{P}) = 0$; b) $P(\text{Tm}) = 0$; $P(\text{P}) = 7.1\%$.

The temperatures are deduced from the polarizations using the formula :

$$P = \tanh(\hbar\omega/2 kT) \quad (18)$$

where ω is the N.M.R. frequency in the given field. The first phase of the evolution involves the convergence of T_{Tm} and T_{P} ; however the asymptote is not $T_{\text{Tm}} = T_{\text{P}}$, but rather $T_{\text{Tm}} = 0.8 T_{\text{P}}$.

At 1.7 tesla (Fig. 5), the thermal mixing tendency is even weaker, since at the end of the first phase, $T_{\text{Tm}} = 0.2 T_{\text{P}}$. At 3.3 tesla, we did not see any mixing effect : the P do not recover after saturation, although the Tm do relax as shown in figure 6.

2.3.2 The rate equations. — To analyse the data and disentangle the role of thermal mixing and spin-lattice relaxation at 0.8 tesla, we introduce as in [21] an intermediate energy reservoir which is coupled to the Tm Zeeman energy Z_{Tm} , to the P Zeeman energy Z_{P} and to the lattice L .

This reservoir \mathcal{H}_{NZ} is the sum of two reservoirs strongly coupled with each other, namely \mathcal{H}_{SS} of the interactions of the electronic spins with themselves and

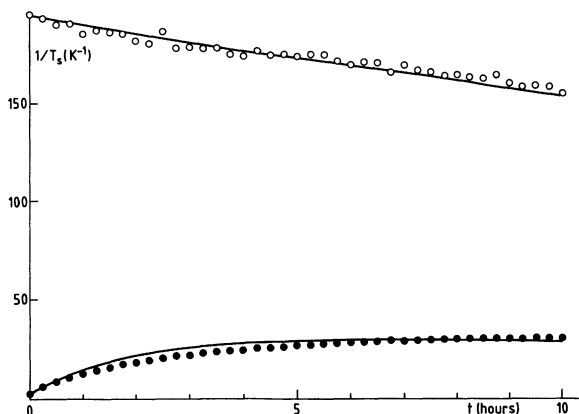


Fig. 5. — Relaxation in 1.7 tesla of the ^{169}Tm (open circles) and ^{31}P (closed circles) inverse spin temperatures $1/T_s$. The initial conditions are : $P(\text{Tm}) = 6.9\%$; $P(\text{P}) = 0$.

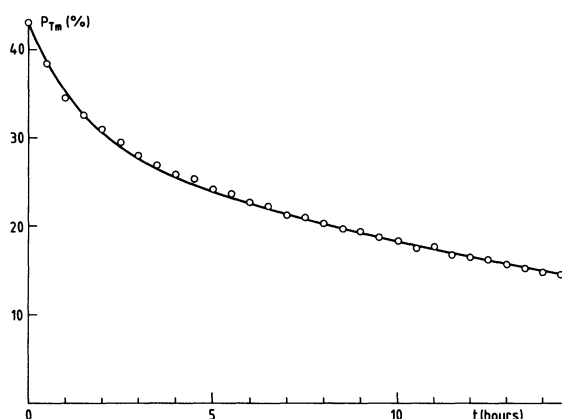


Fig. 6. — Relaxation of the ^{169}Tm polarization in 3.3 tesla.

\mathcal{H}'_{IS} of the interactions of the electronic spins with their neighbouring nuclear spins.

The coupling between \mathcal{H}_{NZ} and Z_{Tm} , Z_{P} and L is governed by three rate equations, depending on three rate constants u , v and R (Fig. 7).

$$\begin{aligned} d\alpha/dt &= -u(\alpha - \delta) \\ d\beta/dt &= -v(\beta - \delta) \\ d\delta/dt &= -u(\delta - \alpha) c_{\alpha}/c_{\delta} - v(\delta - \beta) c_{\beta}/c_{\delta} - R(\delta - \alpha_0). \end{aligned} \quad (19)$$

where α , β , δ and α_0 are the inverse temperatures of Z_{Tm} , Z_{P} , \mathcal{H}_{NZ} and L , and c_{α} , c_{β} , c_{δ} the heat capacities of the first three reservoirs (defined as the derivative of the energy with respect to the inverse temperature).

As usual, it is assumed that $c_{\delta} \ll c_{\alpha}$, c_{β} . The system described by (19) has then a short initial period where only δ changes significantly and leads to a quasi-equilibrium given by :

$$d\delta/dt = 0. \quad (20)$$

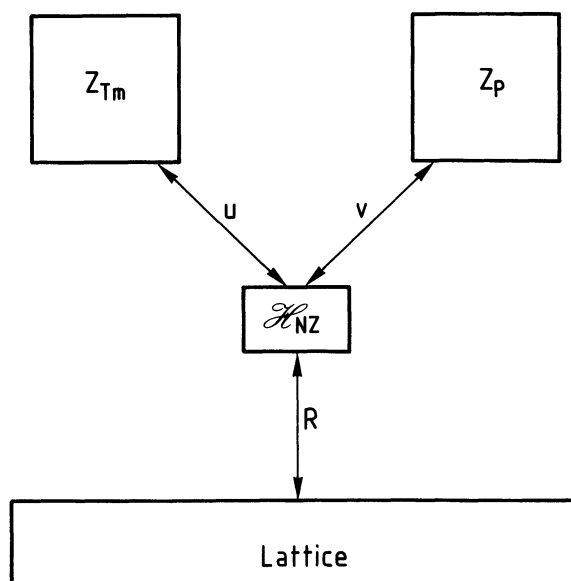


Fig. 7. — Block-diagram of the various energy reservoirs with their mutual couplings. Z_{Tm} = Zeeman reservoir of ^{169}Tm . Z_{P} = Zeeman reservoir of ^{31}P . \mathcal{H}_{NZ} = spin-spin interactions of the paramagnetic impurities.

This gives :

$$\delta = (\alpha u c_{\alpha}/c_{\delta} + \beta v c_{\beta}/c_{\delta} + R \alpha_0)/Z \quad (21)$$

with

$$Z = u c_{\alpha}/c_{\delta} + v c_{\beta}/c_{\delta} + R \quad (22)$$

δ can now be eliminated from (19) which becomes :

$$\begin{aligned} d\alpha/dt &= -w(\alpha - \beta) - u_{\alpha}(\alpha - \alpha_0) \\ d\beta/dt &= -w(\beta - \alpha) c_{\alpha}/c_{\beta} - u_{\beta}(\beta - \beta_0) \end{aligned} \quad (23)$$

with

$$\begin{aligned} u_{\alpha} &= uR/Z \\ u_{\beta} &= vR/Z \\ w &= (w/Z) c_{\beta}/c_{\delta} \end{aligned} \quad (24)$$

u_{α} and u_{β} would be the Tm and P relaxation rates in the absence of the other spin species. w is an effective thermal mixing rate. The general solution of (23) is the sum of two exponentials whose relative amplitudes depend upon the initial conditions.

2.3.3 Discussion. — System (23) correctly describes our experimental results at 0.8 tesla (Fig. 4), taking $u_{\beta} = 0$. The first period of the relaxation does not end with $T_{\text{Tm}} = T_{\text{P}}$ because, contrary to the case of [22], w is not *much* bigger than u_{α} . The smallness of the ratio u_{β}/u_{α} deserves some explanation : the coupling of Z_{Tm} and Z_{P} to \mathcal{H}_{NZ} is caused by electronic « flip-flops » (provided that the electronic impurity concentration is sufficiently high). In the coupling Hamiltonian between nuclei and electrons :

$$\sum_{i\mu} (\gamma_s S^i) A^{i\mu} (\gamma I^{\mu}) \quad (25)$$

the useful terms are of the form :

$$\gamma_s \gamma_{\perp} S_z I_+ \quad \text{or} \quad \gamma_s \gamma_{\perp} S_z I_- \quad (26)$$

The relaxation rate is thus proportional to :

$$\gamma_s^2 \gamma_{\perp}^2 (1 - P_0 P_e) f(\omega) \quad (27)$$

where P_e and P_0 are respectively the actual and thermal equilibrium values of the electronic polarization, and $f(\omega)$ the Fourier transform of the correlation function $F(t)$ of S_z under the effect of the electronic flip-flops [23]. Provided certain approximations are valid (see [23]), the shape function $f(\omega)$ can be taken as a Lorentzian $a/(\omega^2 + a^2)$, of width $a \ll \omega$, so that the relaxation rates u and v are proportional to :

$$\gamma_{\perp}^2 (1 - P_0 P_e) \omega^{-2} \quad (28)$$

where ω is the actual N.M.R. frequency, i.e. $\gamma_{\parallel} H$ when $H \parallel c$ for Tm.

Other terms being equal, the relaxation rate for Tm should be much larger than that of a « normal » nucleus such as P by a factor $(\gamma_{\perp}/\gamma_{\parallel})^2$. It is then not surprising that the ratio $u_{\beta}/u_{\alpha} = u/v$ should be small.

Figure 8 presents the thermal variation of u_{α} and w at 0.8 tesla, between 2 K and 50 mK (in a sample

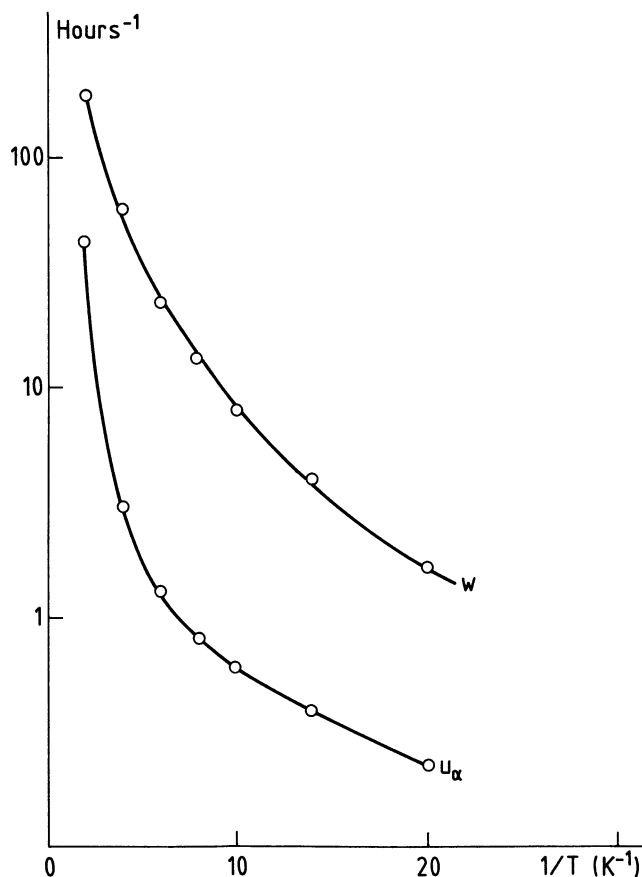


Fig. 8. — Relaxation rate u_{α} and mixing rate w in logarithmics scale, as a function of the reciprocal lattice temperature $1/T$.

different from that used in figure 4, which may explain the slight discrepancies between the two measurements). Both terms contain the factor $1 - P_0 P_e$, so that, in principle, one could deduce from figure 8 the g -factor of the paramagnetic impurities responsible for the relaxation. Owing to the large uncertainties, we can only conclude that it is not incompatible with $g = 1.5$ (the g_{\parallel} value of Yb^{3+}) above 0.2 K. Below 0.2 K, the thermal variation is much slower. We cannot explain this behaviour, which is also observed in many other substances in the dipolar relaxation (CaF_2 , LiF , LiH , ...), or in the mixing rate (LiF , LiH). The novelty of TmPO_4 is that we can observe this anomaly by means of the Zeeman relaxation u_{α} , because it is orders of magnitudes stronger than for « normal » nuclei.

The thermal mixing observed when H is close to the c -axis is also observed in the D.N.P. experiments (see next section). By contrast, we did not observe any mixing with $H \perp c$, either in relaxation or in D.N.P. The reason for this is that when $H \perp c$ the Larmor frequency of Tm is too large and energy exchange is thus impossible between Z_{Tm} and \mathcal{H}_{NZ} . The same consideration applies also at 3.3 T with $H \parallel c$ where there is no observable thermal mixing either.

At 1.7 tesla, we have an intermediate case and, although we did observe some mixing effect (Fig. 5), the results cannot be interpreted completely in terms of system (23). There are certainly other relaxation mechanisms for Tm which unfortunately are not exponential and cannot enter simply into system (23) by a mere modification of u_{α} .

2.4 DYNAMIC NUCLEAR POLARIZATION.

2.4.1. *Paramagnetic impurities.* — The principle of dynamic nuclear polarization (D.N.P.) is well-known : it consists in off-centre E.P.R. saturation by strong microwave irradiation of some paramagnetic impurities the concentration of which should be of the order of 10^{-5} to 10^{-4} with respect to the nuclear spins. X-band E.P.R. studies at 4.2 K revealed the presence of two main types of impurity. Their concentrations were checked by comparison with a small sample of $\text{CuSO}_4 \cdot 5 \text{H}_2\text{O}$, and their g -factors were studied at various angles. For the sample used in our studies, we found :

impurity	g_{\parallel}	g_{\perp}	concentration (per Tm)
1	6.45	4.89	6×10^{-5}
2	1.51	3.2	1×10^{-4}

These were identified as Er^{3+} and Yb^{3+} respectively, since in YPO_4 , one has [24] :

$$\begin{aligned} g_{\parallel} = 6.42 \quad g_{\perp} = 4.81 & \quad \text{for } \text{Er}^{3+} \\ g_{\parallel} = 1.52 \quad g_{\perp} = 3.12 & \quad \text{for } \text{Yb}^{3+} \end{aligned}$$

and very little variation is expected between TmPO_4 and YPO_4 [25]. Furthermore Er and Yb are neighbours of Tm in the periodic table.

2.3.2. Experimental setup. — The apparatus used was the same as that used for nuclear magnetic ordering studies in LiH [26]. In particular, the sample is mounted in a Kel-F sample holder (poly-monochlorotrifluoroethylene) and immersed in the dilute ^3He - ^4He phase of a dilution refrigerator. The lower part of the refrigerator is made of Kel-F tails glued to the metallic upper part by means of epoxy.

The microwave radiation is produced by a 70 GHz carcinotron (a few studies were also made with a 150 GHz carcinotron), and introduced into the ^4He bath near the sample using 8 mm and 4 mm wave guides. It is transmitted by a horn at the end of the waveguide, and irradiates the sample through the various Kel-F layers. This configuration, adapted to neutron diffraction experiments in LiH, is not optimal for all types of D.N.P. experiments, but it was good enough in this case where the limitations to the performance are believed not to arise from cryogenic or microwave power level considerations (see below). The bath temperature was about 80 mK without microwaves. It was calibrated using the N.M.R. signal of Tm in a field of 500 Gauss perpendicular to c [18], where the relaxation time is short even at the lowest sample temperatures, and the signal to noise ratio is very good.

The N.M.R. line of Tm or P was recorded in the following manner : the DC output of a Q -meter, with an appropriate offset, was fed into the input of a multichannel analyser. The latter consists of a card containing analog to digital converters (to digitize the input signal) and digital to analog converters (to visualize the memory content), mounted on a board and added to a PET/CBM computer. 4k-bytes of machine-code subroutines are incorporated in ROM to insure efficient on-line processing, the « friendly » interface with the user being provided by a BASIC program. It is particularly easy to automatize a process with this system, since the multichannel analyser is built inside the microcomputer itself, and since the PET/CBM can be used as a IEEE/488 bus controller.

Linear sweep of the magnetic field is provided by the multichannel analyser itself, operated in the « multiscale » mode : a D/A converter produces a linear ramp, which is the analog output of the channel address. This ramp is fed into a DC power amplifier. The N.M.R. frequency is set so that the resonance occurs in the middle of the first half of the « window » (or « group »), the second half recording only the baseline. Subsequent subtraction of the two halves allows automatic elimination :

- 1) Of the base line,
 - 2) Of the noise due to mains and its harmonics.
- For this purpose, each half-window is composed of

200 channels, and the duration of each channel is set to 500 μs , so that the time lag between corresponding channels of the two groups is 100 ms, i.e. a multiple of the mains period.

2.4.3. Polarization rate. — Only a few attempts were made to polarize with $\mathbf{H} \perp c$, and no significant result were obtained : starting from small polarization, we did observe an increase when we applied the microwave, leading to polarizations of a few %, but this is of the order of the thermal equilibrium polarization. The increase observed probably arose from a shortening of the relaxation time, due to the microwave irradiation : when the latter is applied, the electronic polarization P_e is reduced, and the term $1 - P_0 P_e$ in (28) becomes of order unity, in contrast to its small value when there are no microwaves. It is not surprising that we obtained poor polarizations with $\mathbf{H} \perp c$, since the inhomogeneous broadening of the E.S.R. line is of order 200 Gauss/tesla [18].

On the contrary, with $\mathbf{H} // c$, the Tm polarized efficiently in a time of the order of 10 min, which, considering the electronic concentration used, is very rapid compared to other substances [27]. This efficiency must be attributed to the « anisotropy factor » $A = \gamma_{\perp}/\gamma_{\parallel}$. The equation describing the polarization dynamics has the same form as (24) if the lattice inverse temperature α_0 is replaced by a much higher value, generated by the D.N.P. As discussed in section 2.3.3. above, the relaxation rates u_x and w which appear in (23) are increased by a factor of $(\gamma_{\perp}/\gamma_{\parallel})^2$ with respect to the values typical of isotropic nuclei, leading to relaxation times of a few tens of hours at the lowest temperatures. It is the same factor $(\gamma_{\perp}/\gamma_{\parallel})^2$ which is responsible for the efficiency of the D.N.P. The fact that the polarization rate itself is much shorter than the relaxation rate stems from the increase in the factor $(1 - P_0 P_e)$, itself due to the partial saturation of the E.S.R. line during D.N.P.

2.4.4. Influence of the orientation. — Even with magnetic field roughly parallel to the c -axis, we found that the D.N.P. results were dramatically dependent on the angle θ . First, the « accelerating » factor :

$$(\gamma_{\perp}/\gamma)^2 = A^2(1 + A^2 \tan^2 \theta)^{-1} \quad (28)$$

itself depends rather rapidly on θ . But another effect was found to be even more important : that of the inhomogeneous broadening of the resonance lines.

Figure 9a shows the Tm N.M.R. absorption line (with no dispersion !) after the D.N.P., for a sample with a misalignment θ of = 1 deg. Although the net polarization (as given by the total area of the line) is only 5 %, it is the result of a cancellation of absorptive and emissive parts, each with an area much larger, corresponding to partial polarizations as high as 30 %.

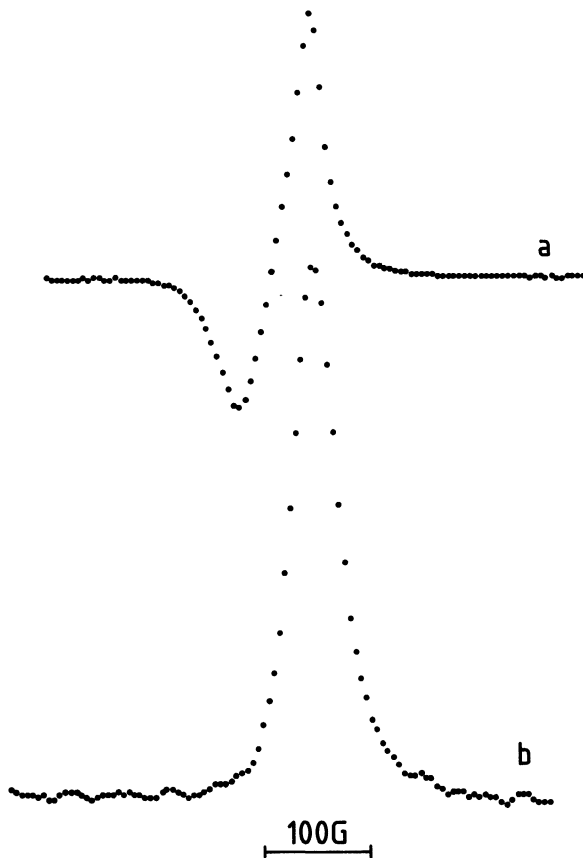


Fig. 9. — N.M.R. lineshape of the ¹⁶⁹Tm after D.N.P. a) in 0.8 tesla with a strong inhomogeneous broadening; b) in 3.3 tesla after cancellation of the inhomogeneous broadening.

A « differential D.N.P. effect » occurs in this case due to the inhomogeneous broadening of the E.S.R. line. The line is composed of a series of « spin packets » relatively decoupled from each other. Let us assume that the microwave frequency is set at the centre of the E.S.R. line, so that some packets are above resonance, and some others are below resonance : the nuclei surrounding the upper packets will tend to polarize positively, and the nuclei surrounding the lower packets will tend to polarize negatively. The resulting average nuclear polarization is then zero, and the N.M.R. absorption signal would be completely flat if it were homogeneous, or even if it suffered an inhomogeneous broadening uncorrelated with the electronic broadening.

Since this is not the case, it must be concluded that the broadening of the E.S.R. line and of the N.M.R. line of Tm are strongly correlated. One possible explanation is the crystalline mosaicity, but as shown by formula (14) of section 2.2.2. (which should apply also to the electronic linewidth), this gives a very small broadening of the E.S.R. lines, since the anisotropy factor *A* is so much smaller for them than for Tm. The only term in (14) which does not depend on *A* is the scatter of the *g*-factors, $\langle \delta\gamma_{\parallel}^2 \rangle^{1/2}/\gamma_{\parallel}$.

If this scatter is due to local strains, it should indeed have a correlated effect on the electronic lines and on the Tm resonance. We saw in section 2.2.2. that for the Tm lines the term $\langle \delta\gamma_{\parallel}^2 \rangle/\gamma_{\parallel}^2$ is negligible. On the other hand, the term $A^2 \theta^2 \langle A^2 \delta\theta^2 \rangle$ in (14) is *not* correlated with the local strains, but with the field inhomogeneity. Hence, there remains for Tm only the term $A^4 \theta^4 \langle \delta\gamma_{\perp}^2 \rangle/\gamma_{\perp}^2$ at $\theta \neq 0$, which indeed is likely to be correlated with the term $\langle \delta\gamma_{\parallel}^2 \rangle/\gamma_{\parallel}^2$ of Yb³⁺. The order of magnitude can be found from examination of figure 10. This figure shows the E.S.R. line of Yb³⁺ at 3.3 tesla (70 GHz), which has a full width at half maximum of 45 Gauss, whereas it is only 10 Gauss at the X band (9 GHz). If we interpret the inhomogeneous broadening by a scattering of *g*_∥, we find a value of $\langle \delta\gamma_{\parallel}^2 \rangle^{1/2}/\gamma_{\parallel}$ of 1.5×10^{-3} for Yb³⁺.

2.4.5. Importance of homogeneity. — For the study of nuclear magnetic ordering, it is of course important to start from a nuclear polarization as high and homogeneous as possible. This is achieved by aligning carefully the field along the *c*-axis. As stated in 2.2.3, the term independent of angle $\langle \delta\gamma_{\parallel}^2 \rangle^{1/2}/\gamma_{\parallel}$ varied from one sample to another and depended on the thermal history of the sample. It was thus necessary to make a number of attempts to obtain the best results. Figure 9b shows the Tm line after such a polarization; it corresponds to a Tm polarization of ≈ 60 %, and the line-width corresponds approximately to its theoretical value, if one takes into account the slight diminution in the second moment when the spins are 60 % polarized.

3. Nuclear magnetic ordering

3.1 GENERAL CONSIDERATIONS. — Henceforth we shall assume that the magnetic field **H**₀ is precisely aligned along the *c*-axis. In any other orientation than this one, the broadening mechanisms discussed in section 2.2 will prevent the observation of an ordered state prepared by the method of A.D.R.F.

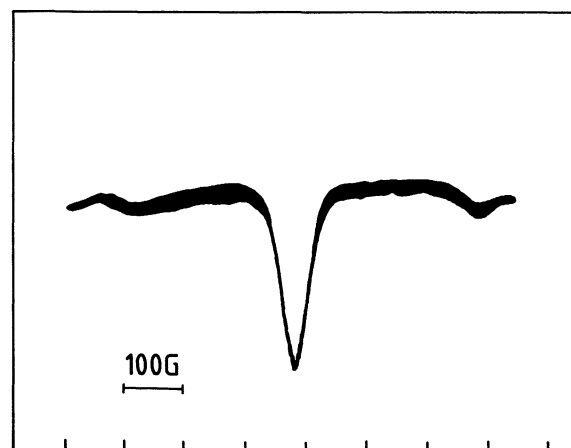


Fig. 10. — E.S.R. line of Yb³⁺ at a frequency of 70 GHz.

In the presence of a strong magnetic field, the Hamiltonian responsible for the ordering is the « truncated dipolar Hamiltonian » which for $\mathbf{H}_0 \parallel c$ takes the form in frequency units :

$$\mathcal{H}'_d = \frac{1}{2} \sum_{i,j} \frac{(1 - 3 \cos^2 \alpha_{ij})}{2 r_{ij}^3} \times \\ \times [2 \gamma_{\parallel}^2 I_z^i I_z^j - \gamma_{\perp}^2 (I_x^i I_x^j + I_y^i I_y^j)], \quad (29)$$

where \mathbf{r}_{ij} is the vector joining spin i and j and α_{ij} its angle with the c -axis taken as the z -axis.

As is usual for a truncated Hamiltonian, the longitudinal components of \mathbf{I} are not coupled to the transverse components. The distinguishing feature of this system is the smallness of the longitudinal terms : the ratio of the transverse and longitudinal components is of order $\left(\frac{\gamma_{\perp}}{\gamma_{\parallel}}\right)^2 = 625$. This feature is attractive because it promotes transverse ordering after demagnetization. In the case of transverse ordering, the equations of motion of the spins include a torque from the external field which induces a precession of the whole structure at the Larmor frequency. Such a rotating structure has already been observed in CaF_2 [3, 28, 29], but in that case the transverse state was degenerate or quasi-degenerate with a longitudinal one. In TmPO_4 the large anisotropy prevents such degeneracy.

From now on, we shall neglect the longitudinal terms of (29) and use the simplified form of \mathcal{H}'_d :

$$\mathcal{H}'_d = -\frac{1}{2} \sum_{i,j} A_{ij} (I_x^i I_x^j + I_y^i I_y^j), \quad (30)$$

with

$$A_{ij} = \frac{\gamma_{\perp}^2}{2} \frac{1 - 3 \cos^2 \alpha_{ij}}{r_{ij}^3}.$$

\mathcal{H}'_d can also be written :

$$\mathcal{H}'_d = \frac{1}{2} \sum_i \omega_i \cdot \mathbf{I}_i$$

with

$$\begin{aligned} \omega_x^i &= - \sum_j A_{ij} I_x^j \\ \omega_y^i &= - \sum_j A_{ij} I_y^j \\ \omega_z^i &= 0. \end{aligned} \quad (31)$$

We now recall briefly how the ordered states of \mathcal{H}'_d may be produced using the method of D.N.P. and A.D.R.F.

When in a field \mathbf{H}_0 the Tm spins are irradiated by an r.f. field \mathbf{H}_1 rotating at frequency ω around \mathbf{H}_0 , their Hamiltonian in a rotating frame which is stationary

with respect to the r.f. field is :

$$\tilde{\mathcal{H}} = \Delta I_z + \mathcal{H}'_d + \omega_1 I_x \quad (32)$$

where $I_z = \sum_i I_z^i$, $I_x = \sum_i I_x^i$

$$\Delta = \gamma_{\parallel} H_0 - \omega \quad \text{and} \quad \omega_1 = \gamma_{\perp} H_1.$$

Equation (32) is the Hamiltonian of a system of spins interacting through \mathcal{H}'_d and experiencing a static field of longitudinal and transverse components $\Delta/\gamma_{\parallel}$ and H_1 respectively. We assume that $H_1 \ll H'_L$ where :

$$H'_L{}^2 = \frac{S_p(\mathcal{H}'_d{}^2)}{\gamma_{\perp}^2 S_p(I_z^2)}.$$

An adiabatic demagnetization analogous to the usual laboratory frame demagnetizations may be performed in the rotating frame by lowering the value of Δ from an initial value $\Delta_{\text{in}} \gg \gamma_{\perp} H'_L$ to the value $\Delta = 0$. When $\Delta = \Delta_{\text{in}}$, $\tilde{\mathcal{H}} \approx \Delta I_z$ and all the entropy is associated with the Zeeman order. When $\Delta = 0$, $\tilde{\mathcal{H}} = \mathcal{H}'_d + \omega_1 I_x \approx \mathcal{H}'_d$ since $H_1 \ll H'_L$, and all the entropy is associated with the dipolar order. Instead of varying Δ , the frequency may be held fixed and the external field H_0 swept. In this case the condition for an adiabatic sweep is [30] :

$$\frac{dH_0}{dt} \ll \gamma_{\perp} H_1^2.$$

This condition ensures conversion of the Zeeman order into dipolar order if the spins are completely isolated from the lattice. In practice, the demagnetization is not perfectly isentropic, as shown later, and dipolar spin lattice relaxation limits to about 10 min the time available after A.D.R.F. for study of the ordered state. On this time scale, Zeeman relaxation can be neglected.

3.2 PREDICTIONS OF THE STABLE STRUCTURES. — Two methods have been used for the prediction of nuclear ordered structures [7, 8], due to Luttinger and Tisza and to Villain. Both methods assume Weiss field expressions for the thermodynamic quantities and proceed by comparing the free energy for all possible structures at a given temperature : the former treats the case $T = 0$ while the latter considers a temperature just below the transition temperature. In the case of TmPO_4 the two methods lead to the same results and we shall concentrate on the Villain method. In TmPO_4 the Tm ions are located on two interpenetrating Bravais lattices labelled 1 and 2 in figure 1. In the following calculation, they are considered as two separate spin systems, in a way similar to that used for the case of two different nuclear species [8]. However, the spins have the same γ , and the Hamiltonian \mathcal{H}'_d contains « flip-flop » terms which do not appear in [8].

We wish to compare the stability of various ordered structures defined by the spatial variation of the nuclear polarization :

$$\mathbf{p}_i = \mathbf{p}(\mathbf{r}_i, T) = 2 \langle \mathbf{I}(\mathbf{r}_i, T) \rangle,$$

and obeying the Weiss field equation

$$\mathbf{p}_i = \frac{\mathbf{H}_i}{H_i} \tanh \left(\frac{\hbar}{2} \beta \gamma_{\perp} H_i \right), \quad (33)$$

where \mathbf{H}_i is the average field at site i and where $\beta = 1/kT$. We shall have occasion to express the Weiss field in frequency units as $\mathbf{h}_i = -\gamma \mathbf{H}_i$: (31) can be reexpressed as :

$$h_x^i = -\frac{1}{2} \sum_j A_{ij} p_x^j \quad (34. a)$$

$$h_y^i = -\frac{1}{2} \sum_j A_{ij} p_y^j \quad (34. b)$$

$$h_z^i = 0. \quad (34. c)$$

The use of (33) amounts to neglecting the short range correlations between spins. The dipolar energy is then equal to $\langle \mathcal{H}'_d \rangle = \frac{1}{4} \sum_i \mathbf{h}_i \cdot \mathbf{p}_i$ and the entropy takes the form :

$$S = N \ln 2 - \sum_i [(1 + p_i) \ln (1 + p_i) + (1 - p_i) \ln (1 - p_i)]. \quad (35)$$

To simplify the problem we assume (following Villain) that we are close to the transition temperature $T_c = 1/k\beta_c$. Then $p_i \ll 1$ and we can expand (33) as :

$$\mathbf{p}_i = -\frac{1}{2} \beta_c \mathbf{h}_i. \quad (36)$$

From (34c) $p_z^i = 0$ and for p_x^i and p_y^i we are left with a set of $2N$ linear equations defined by (34a) (34b) and (36). This set has $2N$ degenerate or non degenerate solutions with different critical temperature T_c . Comparison of the free energies reveals that the stable solution is the one with maximum T_c at $T > 0$ and the one with minimum T_c at $T < 0$. The reader is referred to [7, 8] for the proof.

Having established the formal solution to the problem, we now proceed to determine the explicit form of \mathbf{p}_i using Fourier transformation. The Fourier transforms of the polarizations are defined by :

$$p_x^a(\mathbf{k}) = \frac{1}{\sqrt{N}} \sum_{\mathbf{r}_i^a} p_x^i \exp(i\mathbf{k} \cdot \mathbf{r}_i),$$

where $a = 1, 2$ refers to the two Tm positions. Similar relations hold for the y components. We define the

Fourier transforms of the interaction A_{ij} by :

$$A_{ab}(\mathbf{k}) = \sum_{\mathbf{r}_i^a, \mathbf{r}_j^b} A_{ij} \exp[i\mathbf{k} \cdot (\mathbf{r}_i^a - \mathbf{r}_j^b)],$$

with $a, b = 1, 2$.

By permutation of the indices we obtain :

$$\begin{aligned} A_{11} &= A_{22} = A \\ A_{12} &= A_{21}^* = B. \end{aligned}$$

After Fourier transformation the set defined by (34a) and (36) becomes :

$$\begin{aligned} (A + \lambda) p_x^{(1)}(\mathbf{k}) + B p_x^{(2)}(\mathbf{k}) &= 0 \\ B^* p_x^{(1)}(\mathbf{k}) + (A + \lambda) p_x^{(2)}(\mathbf{k}) &= 0 \end{aligned} \quad (37)$$

with $\lambda = -4/\beta_c$ (38), and we obtain the same system for the y component.

The problem has been considerably simplified since different values of \mathbf{k} do not interfere. For a given value \mathbf{K} of \mathbf{k} , (37) has two solutions :

$$p_x^{(1)} = p_x^{(2)} B/|B| \quad \text{with} \quad \lambda = -A - |B| \quad (39. a)$$

$$p_x^{(1)} = -p_x^{(2)} B/|B| \quad \text{with} \quad \lambda = -A + |B| \quad (39. b)$$

which are degenerate with the solution for $\mathbf{k} = -\mathbf{K}$. The solutions for the y component are exactly the same as for the x component, which yields a further degeneracy. Since $\beta_c = -4/\lambda$, it follows from the free energy criterion mentioned above that the stable solution corresponds to the minimum of $\lambda(\mathbf{k}) = -A(\mathbf{k}) \pm |B(\mathbf{k})|$ at $T > 0$ and to its maximum value at $T < 0$. The solution (39) is in general complex, but thanks to the degeneracy it is always possible to construct a real solution by superposition. Let us assume for example that the stable solutions corresponds to the choice $\lambda(\mathbf{k}_0) = -A(\mathbf{k}_0) - |B(\mathbf{k}_0)|$. Two types of solutions can be constructed :

$$\begin{aligned} p_x^{(1)} &= p \cos(\mathbf{k}_0 \cdot \mathbf{r} + \varphi) & p_x^{(2)} &= p \cos(\mathbf{k}_0 \cdot \mathbf{r} + \varphi + \psi) \\ p_y^{(1)} &= \pm p \sin(\mathbf{k}_0 \cdot \mathbf{r} + \varphi) \\ p_y^{(2)} &= \pm p \sin(\mathbf{k}_0 \cdot \mathbf{r} + \varphi + \psi) \end{aligned} \quad (40)$$

with arbitrary φ and $B/|B| = \exp(-i\psi)$. They correspond to right and left-handed helices of pitch $2\pi/k_0$.

The helical solutions found near T_c remain solutions at lower temperatures. This is a consequence of the fact that p_i is independent of i as well as $h_i = -2p_i/\beta_c$; when β is not close to β_c , (40) is still a solution of (33), provided that p and β are related through :

$$\beta = \beta_c (\tanh^{-1} p)/p. \quad (41)$$

The solutions for which p_i is independent of i are referred to as « permanent » solutions in [7, 8]. As we shall see later, for small values of \mathbf{k} , it is also possible to construct permanent solutions of a variety other than the helical ones.

For the systematic search of the stable structures in TmPO_4 , the values of $\lambda(\mathbf{k})$ have been computed over a set of 4 096 points inside the Brillouin zone. The method for computing the dipolar Fourier transforms is that described in [31]. The minimum of λ corresponding to the solution at $T > 0$ occurs for \mathbf{k} vanishingly small and parallel to \mathbf{H}_0 (the meaning of « vanishingly small » is discussed below). The maximum of λ which gives the solution at $T < 0$ occurs also for small \mathbf{k} values but for \mathbf{k} perpendicular to \mathbf{H}_0 . For $T > 0$ and $T < 0$ the solution is of the type (39a) with B real and of the same sign as A which means that Tm_1 and Tm_2 spins have parallel polarizations.

The case of small values of k deserves special attention. 1) The above calculations fail if k is smaller than $1/R$ where R corresponds to the sample dimensions; otherwise, the Fourier transforms $A_{ab}(\mathbf{k})$ would not be independent of position within the sample. However when k is rigorously zero and the sample is an ellipsoid the A_{ab} 's are independent of position, but depend on the axes ratios of the sample and they can be used to infer the values of $A_{ab}(\mathbf{k})$ when \mathbf{k} lies in the « vanishingly small » domain defined by $1/R \ll k \ll 1/a_0$. If the $A_{ab}(0)$'s are computed for a sphere, it is found in a way equivalent to that of (32) that :

$$\lim_{1/R \ll k \ll 1/a_0} A_{ab}(\mathbf{k}) = A_{ab}(0) + \frac{4\pi}{3} \frac{\gamma_{\perp}^2 \hbar}{a^2 c} (3 \cos^2 \theta_k - 1) \quad (42)$$

where θ_k is the angle between \mathbf{k} and \mathbf{H}' .

2) Since the magnitude of \mathbf{k} does not appear in (42) there is a wide range of k values between $1/R$ and $1/a$ which are quasi degenerate. This means that the pitch of the helix is ill-determined. We shall not enter into the details of what may determine the pitch of the helical structure, but we shall point out that, for small k values, the $A(\mathbf{k})$ degeneracy makes it possible to construct solutions of the form of a ferromagnet with domains. Consider for example the structure of figure 11, where the magnetization is homogeneous

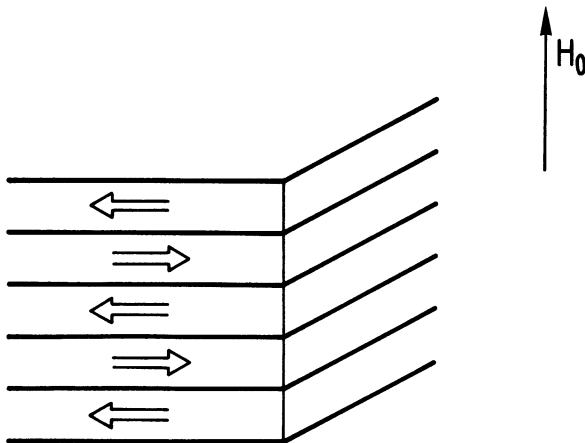


Fig. 11. — Example of a transverse ferromagnetic structure with domains.

inside one domain and points alternately in the positive and negative x -direction. The width d of the domains is chosen so that $a_0 \ll d \ll R$. The Fourier transform of the spatial variation of p consists almost exclusively of components in the range $1/R \ll k \ll 1/a_0$. In consequence, the energy of the structure is (apart from a small correction associated with the presence of domain walls) the same as that of the $T > 0$ helical structure described above. The arrangement of the domains may in practice be much more complex than the simple case we have examined. The domain width and the orientation in the x - y plane of the domain magnetization may vary randomly inside the sample. The only constraints are 1) that the resultant magnetization be zero and 2) that for all the domains $a_0 \ll d \ll R$. The helical structure appears as a particular ferromagnet with domains, in which the domains are very thin and the orientation of the transversal magnetization varies as $\theta = \mathbf{k}_0 \cdot \mathbf{r}$.

We shall assume in what follows that the energy associated with the presence of domain walls prevents the occurrence of a structure with domains and that the solution is always of the helical type : the only experimental justification for this is that the results do not contradict this hypothesis.

To facilitate calculation, we shall assume when necessary that there is a single helix of given pitch $2\pi/k_0$ throughout the sample, although, as stated above, the value of k is only loosely determined as lying within the interval $[1/R, 1/a]$.

3.3 MAIN PROPERTIES OF THE ORDERED STATE. — Our calculations yield the following results :

— Critical temperatures :

At $T > 0$ $\lambda_{\min} = -A(\mathbf{k}_0) - B(\mathbf{k}_0)$ with \mathbf{k}_0 small and parallel to \mathbf{c} ; $A(\mathbf{k}_0) = 18,7 \gamma_{\perp}^2 \hbar/2 a_0^3$; $B(\mathbf{k}_0) = 27,4 \gamma_{\perp}^2 \hbar/2 a_0^3$. At $T < 0$ $\lambda_{\max} = -A(\mathbf{k}_0) - B(\mathbf{k}_0)$ with \mathbf{k}_0 small and perpendicular to \mathbf{c} ; $A(\mathbf{k}_0) = -10 \gamma_{\perp}^2 \hbar/2 a_0^3$; $B(\mathbf{k}_0) = -1,3 \gamma_{\perp}^2 \hbar/2 a_0^3$.

The positive and negative critical temperature are deduced from λ_{\min} and λ_{\max} using (38) which yields :

$$T_c = + 4.22 \mu\text{K}$$

$$T_c = - 1.03 \mu\text{K}.$$

— Critical entropy :

In our experiment TmPO_4 is not prepared at a particular temperature but rather at a given entropy which is related to the polarization P_{in} prior to demagnetization by (35), with p_i replaced by P_{in} . We thus concern ourselves with the critical polarization p_c which leads to the critical temperature after demagnetization. The value of p_c cannot be deduced from the Weiss field approximation since the latter assumes a critical entropy $S_c = N \ln 2$ which would give $p_c = 0$. A more realistic value of S_c is obtained if we assume that the high temperature expansion for the entropy :

$$S = N(\ln 2 - \beta^2 \hbar^2 \gamma_{\perp}^2 H_L'^2/4)$$

is still valid at the transition temperature. It is easy to show then that

$$p_c = \gamma_{\perp} H'_L / \lambda.$$

For $H_0 \parallel c$, $H'_L = 1.36$ G which gives :

$$p_c = 20.4 \% \text{ at } T > 0$$

$$p_c = 83.3 \% \text{ at } T < 0.$$

— Internal fields :

The Weiss fields at absolute zero are obtained from (36) by making $p_i = 1$:

$$\text{at } T > 0 \quad h_i = 176 \text{ kHz whence } H_i = 6.4 \text{ G}$$

$$\text{ar } T < 0 \quad h_i = 43 \text{ kHz whence } H_i = 1.6 \text{ G}.$$

— Susceptibility and helimagnetic resonances :

We now consider the response of the Tm spins to a small field $H_1 = \omega_1 / \gamma_{\perp}$ directed perpendicularly to H_0 and rotating at frequency ω in the laboratory frame (or $\Delta = \omega_0 - \omega$ in the frame rotating at the Larmor frequency). When $\Delta = 0$, H_1 appears static in the rotating frame; moreover, it does not perturb the equilibrium reached at the end of the demagnetization, because the latter terminated at the same frequency $\omega = \omega_0$. There is no energy transfer between the r.f. field and the Tm spins : the response of the Tm is thus purely dispersive, which means that they develop a resultant polarization \bar{p}_i parallel to H_1 . We can define a real susceptibility $\chi_{\perp}(0)$ by $\chi_{\perp}(0) = \bar{p}_i / \omega_1$.

When $\Delta \neq 0$, $\chi_{\perp}(\Delta)$ is complex and, as shown below, it exhibits resonances analogous to the ferromagnetic and antiferromagnetic resonances. We present here a simplified derivation of the response of the spins to an r.f. field. This derivation rests on two properties :

Property 1 : The presence of H_1 does not change the parallelism of the polarizations of Tm 1 and 2. We can thus study the motion of the \mathbf{p}_i 's without specifying label 1 or 2.

Property 2 : Although the action of H_1 may create harmonics of the \mathbf{k}_0 wave vector, the variation of \mathbf{p}_i remains smooth on the scale of the interatomic spacing.

We may describe the dipolar couplings between the different Tm spins by writing for each spin i a generalized Bloch equation in the frame rotating at the Larmor frequency :

$$\dot{\mathbf{p}}_i = \mathbf{p}_i \wedge \gamma \mathbf{H}(t), \quad (43)$$

where $\mathbf{H}(t)$ is the sum of the instantaneous internal field \mathbf{H}_i and of $\mathbf{H}_1(t)$. The fact that the gyromagnetic tensor γ multiplies $\mathbf{H}(t)$ rather than \mathbf{p}_i is justified in [16]. The components of $\mathbf{h}_i = -\gamma \mathbf{H}_i$ as a function of the instantaneous \mathbf{p}_i are given by (34). The assumption of a smooth variation of \mathbf{p}_i implies that its Fourier transform has only components in the range $[1/R, 1/a]$, except for the $\mathbf{k} = 0$ component associated with the average $\bar{\mathbf{p}}_i$ of \mathbf{p}_i . By virtue of the degeneracy of the

$A(\mathbf{k})$'s, we can write :

$$h_x^i = D(k_0) (p_x^i - \bar{p}_x^i) + D(0) \bar{p}_x^i = -qp_x^i + r\bar{p}_x^i$$

$$h_y^i = D(k_0) (p_y^i - \bar{p}_y^i) + D(0) \bar{p}_y^i = -qp_y^i + r\bar{p}_y^i$$

$$h_z^i = 0$$

with : $D(\mathbf{k}) = A(\mathbf{k}) + B(\mathbf{k})$

$$q = -D(\mathbf{k}_0)$$

$$r = D(0) - D(\mathbf{k}_0).$$

From now on, we drop the index i for brevity and introduce :

$$p_+ = p_-^* = p_x + ip_y.$$

The three components of (43) can be recast in the compact form :

$$\begin{aligned} \dot{p}_+ &= -i\omega_+ p_+ \\ \dot{p}_- &= i\omega_- p_- \\ \dot{p}_z &= \frac{i}{2}(\omega_+ p_- - \omega_- p_+), \end{aligned} \quad (44)$$

with $\omega_+ = \omega_-^* = -qp_+ + rp_+ + \omega_1 \exp(i\Delta t)$.

As usual, we linearize (44) by assuming that p_+ and p_- depart only slightly from their equilibrium values p_+^0 and p_-^0 . We define ε_+ and ε_- by :

$$p_+ = p_+^0 + \varepsilon_+ \quad p_- = p_-^0 + \varepsilon_-$$

and we note that :

$$\overline{p_+^0} = \overline{p_-^0} = \overline{p_+^0 p_+^0} = \overline{p_-^0 p_-^0} = 0$$

and $\overline{p_+^0 p_-^0} = p_1^2$.

In (44) we retain only the terms which are linear in ω_1 , in p_z and in the ε 's. This yields :

$$\dot{\varepsilon}_+ = iqp_+^0 p_z \quad (45. a)$$

$$\dot{\varepsilon}_- = -iqp_-^0 p_z \quad (45. b)$$

$$\begin{aligned} \dot{p}_z &= i/2 \omega_1 (p_-^0 \exp(i\Delta t) - p_+^0 \exp(-i\Delta t)) + \\ &+ r\bar{\varepsilon}_+ p_-^0 - r\bar{\varepsilon}_- p_+^0. \end{aligned} \quad (45. c)$$

It is necessary to calculate the average values $\bar{\varepsilon}_+$ and $\bar{\varepsilon}_-$ which will give the average transversal polarizations \bar{p}_x and \bar{p}_y through :

$$\bar{p}_x = \frac{\bar{\varepsilon}_+ + \bar{\varepsilon}_-}{2}, \quad \bar{p}_y = \frac{\bar{\varepsilon}_+ - \bar{\varepsilon}_-}{2i}.$$

We remark that $\dot{\bar{p}}_z = 0$ and, since $\bar{p}_z = 0$ at $t = 0$, $\bar{p}_z = 0$ at all time. (45. a) yields :

$$\dot{\bar{\varepsilon}}_+ = iqp_+^0 p_z. \quad (46)$$

By multiplying both sides of (45.c) by p_+^0 and taking the average we get :

$$\overline{p_+^0 p_z} = i/2 p_+^2 (\omega_1 \exp(i \Delta t) + r \varepsilon_+). \quad (47)$$

The solution of (46) and (47) is :

$$\bar{\varepsilon}_+ = q p_+^2 \omega_1 \exp(i \Delta t) / (2 \Delta^2 - r q p_+^2)$$

and we have $\bar{\varepsilon}_- = (\varepsilon_+)^*$.

$\chi_{\perp}(0)$ is thus equal to :

$$\chi_{\perp}(0) = \frac{\bar{\varepsilon}_+(0) + \bar{\varepsilon}_-(0)}{2 \omega_1} = -\frac{1}{r} = \frac{1}{D(\mathbf{k}_0) - D(0)} \quad (48)$$

$\bar{\varepsilon}_+$ and $\bar{\varepsilon}_-$ have two resonance frequencies given by :

$$\Omega = \pm p_{\perp} \sqrt{\frac{qr}{2}}. \quad (49)$$

The positive and negative sign of Ω correspond respectively to absorption and emission, as can be seen from the sign of $\bar{p}_y = (\bar{\varepsilon}_+ - \bar{\varepsilon}_-) / 2i$.

3.4 EXPERIMENTAL RESULTS. — The experiments were conducted in a field $H_0 = 3.3$ T, this being the field where the best D.N.P. results were obtained : to wit a Tm polarization $P_{in} = 60\%$. For the study of magnetic ordering it is convenient to work in high fields, because this affords longer relaxation times. On the other hand H_0 should not be too high in order to keep the inhomogeneous Tm broadening within reasonable limits and also because the maximum field angle correction which may be applied with our compensating coils falls as $1/H_0$. It is convenient to keep a fixed value of field throughout the experiment and we finally compromised on a value of 3.3 T. At this field the linewidth is 60 Gauss, whereas the calculated homogeneous width is 30 Gauss and at 100 mK, the Tm Zeeman relaxation time is 20 h and the dipolar relaxation time 11 min. We have tested the efficiency of the Adiabatic Demagnetization by means of a cycle in which an A.D.R.F. is immediately followed by a remagnetization. Under ideal conditions of complete adiabaticity and no relaxation this cycle should leave the polarization unchanged. With $H_1 = 50$ mG a sweep rate $dH_0/dt = 0.5$ G/s we find $\Delta p/p = 10\%$. We assume that this represents twice the irreversibility of a single A.D.R.F.

This irreversibility is presumably caused by both an irreversible mixing of the Zeeman and dipolar energies when the RF reaches the wings of the N.M.R. and dipolar relaxation during A.D.R.F. due to the shortness of T_{1d} . Another consequence of the short T_{1d} is that it reduces the time available for study of the ordered state, but this is partly offset by the rapidity of D.N.P. which shortens the delay between successive demagnetizations. The experimental observations are of two kinds : the first use Tm-N.M.R. and the second involve

Tm-P double resonance which is detected by its effect on the P-N.M.R.

3.4.1 Results of the Tm-N.M.R. study. — In section (3.2), we concluded that an initial polarization $P_{in} > 20\%$ and $P_{in} > 82\%$ is required to reach the ordered states at $T > 0$ and $T < 0$ respectively. Given an initial polarization of 60%, we may thus observe only the positive temperature ordered state. The Tm signals following A.D.R.F. are shown in figure 12. It is clear that the shape of the positive temperature signal at $t = 0$ differs much more from that of the final paramagnetic signal than it does at negative temperature. The paramagnetic signal does not contain any sharp resonance features (since the paramagnetic state corresponds to a random distribution of internal fields). On the contrary, the signal of figure 12a has two distinct resonances symmetric with respect to the Larmor frequency. Quantitative analysis of the Tm signals yields the following properties :

3.4.1.1 Measurement of the dipolar energy. — The Tm spin temperature T cannot be deduced from the Tm signals, but the Tm dipolar energy $\langle \mathcal{H}'_d \rangle$ may be computed from the first moment M_1 of the absorption line. Since $\langle \mathcal{H}'_d \rangle$ varies monotonically with T it is used as a parameter against which the observed quantities are plotted.

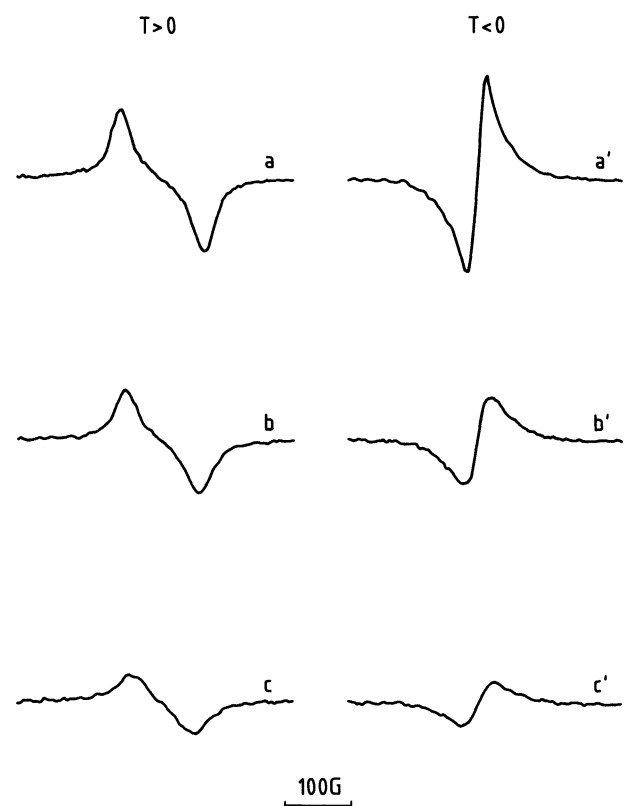


Fig. 12. — N.M.R. absorption signals of ^{169}Tm for both signs of temperature at different time t after the end of the A.D.R.F. : a and a' : $t = 0$; b and b' : $t = 4$ min; c and c' : $t = 11$ min.

In [8, 33] it is shown that :

$$M_1 = \frac{\pi}{2} \omega_1 \xi \langle [I_-, [I_+, \mathcal{H}'_d]] \rangle_0,$$

where $\langle \ \rangle_0$ means thermal average and where ξ is a calibration constant which depends upon the gain of the spectrometer. The product $\omega_1 \xi$ also appears in the relation between the polarization of the Tm spins and the area of their absorption signal; thus, when the N.M.R. spectrometer is calibrated for the measurement of polarizations (by the usual procedures), it is calibrated at the same time for the measurement of dipolar energies. The double commutator should be evaluated with the particular form (30) of \mathcal{H}'_d . It is easily shown that :

$$[I_-, [I_+, \mathcal{H}'_d]] = 2 \mathcal{H}'_d + \text{longitudinal terms}.$$

Owing to the particular form of \mathcal{H}'_d , the expectation value of the longitudinal terms vanishes, whence :

$$M_1 = \pi \omega_1 \xi \langle \mathcal{H}'_d \rangle.$$

3.4.1.2 Measurement of $\chi_{\perp}(0)$. — As defined in section (3.3), $\chi_{\perp}(0)$ measures the dispersive response to a transversal field at the Larmor frequency and can be deduced from the absorption signal using the Kramers-Krönig relations. $\chi_{\perp}(0)$ and $\langle \mathcal{H}'_d \rangle$ have been computed from the digitized signals by means of the C.B.M. microcomputer (see Sect. 2.4.2) and the results at $T > 0$ and $T < 0$ are shown in figure 13 together with the estimated uncertainties and with the Weiss field values (48) of $\chi_{\perp}(0)$ in the predicted ordered state. For the value of $D(0)$ in (48), we have taken the value -15 kHz for a prolate ellipsoid of axis ratio 4.4 which approximates roughly to the somewhat irregular shape of our sample.

At $T > 0$, $\chi_{\perp}(0)$ reaches a value close to the theoretical value and is nearly constant at high values of $\langle \mathcal{H}'_d \rangle$. This indicates that an ordered state is obtained as was suggested by the shape of the signal. At $T < 0$, $\chi_{\perp}(0)$ increases even for the largest value of $\langle \mathcal{H}'_d \rangle$, and the Weiss field value is not reached.

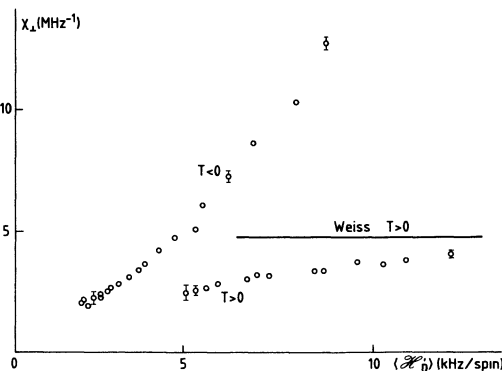


Fig. 13. — Transverse susceptibility of ¹⁶⁹Tm as a function of dipolar energy for both signs of temperature.

3.4.1.3 Helimagnetic resonances. — The Tm signal after demagnetization at $T > 0$ shows two well separated peaks at ± 72 kHz from the Larmor frequency (Fig. 12a). The shape of the signal is not a test of the predicted structure since a variety of different structures yield similar shapes. However, one test is to compute the value of p_{\perp} which, inserted in (49) together with $D(0) = -15$ kHz gives $\Omega = \pm 72$ kHz. One finds $p_{\perp} = 61\%$ which is close to our starting polarization of about 60%.

3.4.1.4 Discussion of the Tm-N.M.R. study. — If we use $p_{\perp} = 60\%$ in the Weiss field expression of the dipolar energy we find a value of $\langle \mathcal{H}'_d \rangle = -15.8$ kHz/spin; to this value must be added the negative contribution of the short range correlations which are overlooked by the Weiss field approximation. An estimate of this contribution can be obtained from the high temperature expansion :

$$\langle \mathcal{H}'_d \rangle = -16.9 \times 10^{-6} \times \frac{1}{T} \text{ kHz/spin} \quad (50)$$

by considering that, at the transition ($T = 4.22$ μ K), all the dipolar energy is short ranged, and by assuming that the short range contribution at the lowest temperature is still the same as at the transition. This gives a short range contribution of -4 kHz/spin immediately after the A.D.R.F. : from the measured total energy of -12.2 kHz/spin we deduce a long range, Weiss field value of -8 kHz/spin, two times lower than our prediction of -15.8 kHz/spin. To reconcile the two figures, we should assume a transverse polarization of only 42% which is substantially smaller than the value computed from the position of the peaks of the Tm N.M.R. signal. We have no clear cut explanation to this discrepancy. Up to now, the results obtained are in qualitative agreement with the predicted transverse structure, but they are not peculiar to transverse ordering since similar results are obtained with longitudinal ordering (see for instance [8] page 546 and 547). In the next section, we present an experiment which proves that the Tm spins are definitely not quantized along the external magnetic field.

3.4.2 The ³¹P-N.M.R. study. — As mentioned above, the transverse helical structure is characterized by an internal rotating field H_i of several Gauss which might seem easy to detect. In practice, detection on a macroscopic scale is impossible because all directions of transverse magnetization are represented in the helical structure, and there is overall cancellation. This necessitates the use of a microscopic probe, hence our observation of P-N.M.R. The existence of transverse ordering does not influence directly the P line shape but can be revealed by a double resonance experiment already used in CaF₂ [3]. The gist of the method consists in using the transverse rotating Weiss field experienced by the Tm spins in place of an externally

applied r.f. field, for a Hartmann-Hahn-like resonant thermal mixing between Tm and P spins. More precisely, the P spins (referred to as spins S) are irradiated by an rf field $H_1 = \omega_{1s}/\gamma_s$ applied at a frequency $\omega = \omega_s - \Delta$ close to their Larmor frequency but with $\Delta \gg \omega_{1s}$ so that the effective field \mathbf{H}_e is very nearly parallel to \mathbf{H}_0 . The peculiarity of the experiment is that, contrary to a usual double resonance experiment, it is not necessary to apply a second external r.f. field close to the Larmor frequency ω_1 of Tm (referred to as spins I). This role is played by the internal Weiss field H_i itself. For the sake of simplicity, H_i may be thought of as an external r.f. field. The conditions then resemble those of the classical case studied by Hartmann and Hahn [34], who showed that such a double irradiation produces simultaneous Tm-P transitions in which a flip-flop occurs between a Tm spin quantized along \mathbf{H}_i and a P spin quantized along \mathbf{H}_e (i.e. very nearly along \mathbf{H}_0). The most important point is that the double resonance process is resonant when $\Delta = \gamma_\perp H_i$, and not only may the observation of such a resonance condition in TmPO_4 be interpreted as evidence for the existence of an internal rotating field, but in addition it provides a means of measuring this field. We examine now more precisely the details of the transitions, and, to pursue the analogy with the Hartmann-Hahn experiment, we write the Hamiltonian of a Tm spin i in the ordered state in a frame rotating at frequency ω_i in the form :

$$\tilde{\mathcal{H}} = \gamma_\perp H_i I_x^i + \delta,$$

where the first term is the Zeeman interaction of spin i with the Weiss field \mathbf{H}_i (directed in the x direction), and where δ is a random Hamiltonian which represents phenomenologically the dipolar short range order of Tm. For P we use a second frame rotating at frequency ω ; the Hamiltonian for a system consisting of one Tm spin i plus one P spin ν is then :

$$\tilde{\mathcal{H}} = \gamma_\perp H_i I_x^i + \delta + \Delta S_z^\nu + \omega_{1s} S_x^\nu + \mathcal{H}'_{IS}, \quad (51)$$

where \mathcal{H}'_{IS} is the part of the Tm-P interaction \mathcal{H}_{IS} which commutes with \mathbf{I} and \mathbf{S} . All the other terms of \mathcal{H}_{IS} give terms oscillating at frequency ω and 2ω and their contributions to the transition probability are thus negligible.

\mathcal{H}'_{IS} is of the form :

$$\mathcal{H}'_{IS} = B_{iv} I_z^i S_z^\nu.$$

We assume that the mutual P interactions are much smaller than the P Zeeman energy in the rotating frame. Under this condition, the different P spins can be considered as independent, and we can speak of the transition probability of a single P spin.

Since we assumed that $\Delta \gg \omega_1$ we can write :

$$\Delta S_z^\nu + \omega_1 S_x^\nu \approx \Delta S_z^\nu,$$

where the direction of quantization Z makes a small angle $\theta \approx \frac{\omega_{1s}}{\Delta}$ with the direction z of \mathbf{H}_0 . We have :

$$S_z^\nu = \cos \theta S_z^\nu - \sin \theta S_x^\nu,$$

and we see that \mathcal{H}'_{IS} contains a part V :

$$V = -\sin \theta B_{iv} I_z^i S_x^\nu \quad (52)$$

which commutes neither with $\gamma_\perp H_i I_x^i + \delta$ nor with ΔS_z^ν , and produces the Tm-P transitions with a rate $W = \sin^2 \theta f(\Delta)$. The resonant dependence of $f(\Delta)$ on Δ results from a simple energy conservation argument : the Hamiltonian $\tilde{\mathcal{H}}$ in the doubly rotating frame is time-independent, and the transitions induced by V must conserve energy in this frame. The reversal of a P spin changes the energy by an amount Δ . The average change due to a Tm spin reversal is $\gamma_\perp H_i$ with some dispersion due to the effect of δ . In the ordered state, $f(\Delta)$ thus peaks at :

$$\Delta = \gamma_\perp H_i. \quad (53)$$

In the paramagnetic state the Weiss term $\gamma_\perp H_i I_x^i$ disappears from (51) and the energy conserving processes are centred about $\Delta = 0$.

In section (3.5), we shall give a more rigorous treatment of the ordered case, and we shall relate the width of the peak of $f(\Delta)$ to the dispersion of the spin wave spectrum.

We show now how the Tm-P transitions affect the Tm and P observables and how they can be detected. Under the influence of the term V , the Tm-P Hamiltonian (51) evolves towards an equilibrium state where the Tm dipolar interactions \mathcal{H}'_d and the P effective Zeeman interaction ΔS_z have a common temperature T_f . As a consequence, there is a change of the Tm dipolar energy $\langle \mathcal{H}'_d \rangle$ and of the effective P Zeeman energy $\Delta \langle S_z \rangle$. The first experimental problem is to adjust the length Δt of irradiation at $\omega_s - \Delta$: if Δt is too small, no measurable variation of $\langle \mathcal{H}'_d \rangle$ and $\Delta \langle S_z \rangle$ will be produced ; if Δt is too long the variation of $\langle \mathcal{H}'_d \rangle$ will be large and the ordered state will be destroyed. Once Δt has been fixed, the problem is to detect the variation of $\langle \mathcal{H}'_d \rangle$ or $\Delta \langle S_z \rangle$.

That the P irradiation can produce a large variation of $\langle \mathcal{H}'_d \rangle$ if its duration is too long, is shown by the following example. We assume that the P are initially unpolarized and that the irradiation is long enough to lead to complete equilibrium. Before and after irradiation, $\langle \mathcal{H}'_d \rangle$ is respectively equal to $\langle \mathcal{H}'_d \rangle_{in}$ and $\langle \mathcal{H}'_d \rangle_f$; the P polarization varies from 0 to p_{eq} . The values of Δ/γ_s in our experiment lie between 10 G and 100 G which implies $\Delta S_z \gg \mathcal{H}'_{IS}$. To a good approximation p_{eq} is then given by :

$$p_{eq} = \tanh(\hbar \Delta / 2 k T_f). \quad (54)$$

Similarly we can estimate the value of $\langle \mathcal{H}'_d \rangle$ from the

Weiss field expressions which give $\langle \mathcal{H}'_d \rangle = -\frac{1}{4}N\gamma_\perp H_i p_\perp$ with $p_\perp = \tanh\left(\frac{\hbar\gamma_\perp H_i}{2kT_f}\right)$. Since $\Delta \approx \gamma_\perp H_i$ we have $p_\perp \approx p_{eq}$, and, since the number N of Tm spins is equal to the number of P spins, we find that :

$$\langle \mathcal{H}'_d \rangle_f \approx \frac{1}{4} \Delta p_{eq} = \frac{1}{2} \Delta \langle S_z \rangle.$$

The total energy $\langle \mathcal{H}'_d \rangle + \Delta \langle S_z \rangle$ must be the same before and after irradiation. This leads to :

$$\langle \mathcal{H}'_d \rangle_f \approx \frac{1}{3} \langle \mathcal{H}'_d \rangle_{in}$$

which means that complete equilibrium under P irradiation leads to almost complete disappearance of the Tm dipolar energy. In order to make a non destructive measurement of W we must irradiate for a time $\Delta t \ll \frac{1}{W}$, so that the spins are only slightly displaced towards equilibrium. This should be contrasted with the case of CaF₂, where the ordered spins I are those of ¹⁹F and the spins S are those of the rare isotope ⁴³Ca. There, complete equilibrium between the I and S systems does not suppress the ¹⁹F order.

In practice, the experiment is performed as follows :

1) The P polarization is saturated.

2) The P are irradiated at frequency $\omega_s - \Delta$. The r.f. field amplitude is $H_1 = 0.68$ G and $\Delta t = 1$ s or 3 s. Under these conditions and for $10 \text{ G} \ll \frac{\Delta}{\gamma_s} \ll 100 \text{ G}$, the condition $\Delta t \ll 1/W$ is always satisfied. We have also checked that the thermal heat input to the sample is small enough to keep a low sample temperature and a long T_{1d} .

3) $\langle \mathcal{H}'_d \rangle$ and the P polarization p are measured.

The operations 1, 2, 3 are repeated with a new value of Δ . Since $\langle \mathcal{H}'_d \rangle$ is measured before and after each irradiation we can check that its variation $\delta \langle \mathcal{H}'_d \rangle$ is small. It can be shown (see Sect. 3.5), starting from very general assumptions that the polarization of the P spins grows exponentially at a rate W . Since $\Delta t \ll 1/W$, W is related to p by :

$$W = \frac{1}{\Delta t} \frac{p}{p_{eq}},$$

whence

$$f(\Delta) = (\Delta/\omega_1)^2 \frac{1}{\Delta t} \frac{p}{p_{eq}}. \quad (55)$$

Because of the conservation of energy we have also

$$W = \frac{1}{\Delta t} \frac{\delta \langle \mathcal{H}'_d \rangle}{\langle \mathcal{H}'_d \rangle}.$$

The measurement of W using the variation of

$\langle \mathcal{H}'_d \rangle$ would require a very good signal to noise ratio since W causes a small variation $\delta \langle \mathcal{H}'_d \rangle$ in a large quantity $\langle \mathcal{H}'_d \rangle$. It is preferable to saturate the P spins beforehand and measure then the small P polarization produced by the irradiation. Another advantage of this procedure lies in the fact that the P polarization does not vary due to relaxation (see Sect. 2.3), contrary to $\langle \mathcal{H}'_d \rangle$.

p_{eq} is difficult to measure because the time taken to reach equilibrium is very long. We therefore define a new quantity

$$g(\Delta) = p_{eq} f(\Delta) = \left(\frac{\Delta}{\omega_1}\right)^2 \frac{p}{\Delta t}$$

which is more directly related to the experimentally measured quantities. From the values of $g(\Delta)$, approximate values of $f(\Delta)$ may be deduced by making reasonable assumptions about the values of p_{eq} . In the ordered state $g(\Delta)$ can be directly compared to theoretical predictions (see Sect. 3.5) and the comparison is not affected by the uncertainty in p_{eq} .

Figure 14 shows the values of $g(\Delta)$ measured for various values of $\langle \mathcal{H}'_d \rangle$. The increase of $g(\Delta)$ with $\langle \mathcal{H}'_d \rangle$ and the shift of the peak position toward large values of Δ is consistent with our explanation above, and also with the more sophisticated analysis to be presented below. But $g(\Delta)$ presents a peak even in the paramagnetic state : for a complete proof of the transverse character of the structure we should show that, when the values of $g(\Delta)$ are converted into values of $f(\Delta)$, there is still a peak of $f(\Delta)$ in the ordered state and none in the paramagnetic state. This is done as follows : in the ordered state we can take as an estimate of the Tm temperature T the value which gives $p_\perp = 61\%$ according to (41); in the paramagnetic state we can take the value which gives the measured value of $\langle \mathcal{H}'_d \rangle$ according to the high temperature expansion (50). This gives $T = 3.6 \mu\text{K}$ in the first case and $T = 7.6 \mu\text{K}$ in the second. With these values of T , we can compute p_{eq} from (54) and $f(\Delta)$ from (55). The result is shown in figure 15 : the peak can still be seen for $\langle \mathcal{H}'_d \rangle = -11 \text{ kHz/spin}$

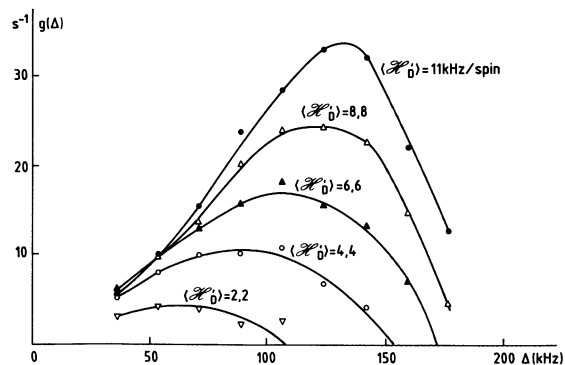


Fig. 14. — Weighted mixing rate $g(\Delta)$ as a function of the distance Δ to resonance, for various dipolar energies $\langle \mathcal{H}'_d \rangle$.

but not when $\langle \mathcal{H}'_d \rangle = -2.2$ kHz/spin. The result in the ordered state does not depend of the particular choice of T : a much higher value would be needed to suppress the peak of $f(\Delta)$. Although there is some uncertainty on the value of p_\perp it should be mentioned that formula (41) tends to overestimate T , since the correlations tend to diminish the order parameter at a given temperature. The peak of $f(\Delta)$ occurs at $\Delta = 130$ kHz, which, according to (53), corresponds to an internal field $H_i = 4.7$ G and a transverse polarization $p_\perp = 73\%$. This is not realistic since it is larger than P_{in} . A more elaborate analysis of the peak shape and position given in next section leads to a somewhat lower value.

3.5 ANALYSIS OF THE DOUBLE RESONANCE EXPERIMENT WITHIN THE R.P.A. APPROXIMATION. — In the previous section we assumed that, in the double resonance experiment, a single spin of Tm is reversed with a consequent change in energy of $\gamma_\perp H_i$. In fact, the true Tm excitations are spin waves of wave vector \mathbf{k} and energy $\omega(\mathbf{k})$. The dispersion of $\omega(\mathbf{k})$ gives rise to a spread in the resonance condition (53) which is now replaced for a given mode \mathbf{k} by $\Delta = \omega(\mathbf{k})$.

The purpose of this section is first to establish the energy and form of the spin waves, and then to derive the coupling between a P spin and a Tm spin wave. The method used is very similar to that of [28, 29].

3.5.1 The spin wave excitations of the helical structure. — We assume an helical structure of pitch $2\pi/k_0$. The components of the Tm polarization vary as :

$$\begin{aligned} p_x^i &= \cos \mathbf{k}_0 \cdot \mathbf{r}_i \\ p_y^i &= \sin \mathbf{k}_0 \cdot \mathbf{r}_i \\ p_z^i &= 0. \end{aligned}$$

We introduce for each spin i a new set of axis defined by the transformation :

$$\begin{aligned} I_x^i &= \cos \theta_i I_z^i + \sin \theta_i I_y^i \\ I_y^i &= -\sin \theta_i I_z^i + \cos \theta_i I_x^i \\ I_z^i &= -I_x^i \end{aligned} \quad (56)$$

with $\theta_i = \mathbf{k}_0 \cdot \mathbf{r}_i$.

Each spin i is now quantized along the Z direction and \mathcal{H}'_d takes the form :

$$\begin{aligned} \mathcal{H}'_d &= \frac{1}{2} \sum_{i,j} A_{ij} \left[-c_{ij} I_z^i I_z^j + \right. \\ &\quad - \left(\frac{c_{ij}}{4} \right) (I_+^i I_-^j + I_-^i I_+^j) \\ &\quad + \left(\frac{c_{ij}}{4} \right) (I_+^i I_+^j + I_-^i I_-^j) \\ &\quad \left. + \frac{1}{2i} s_{ij} [I_z^i (I_+^j - I_-^j) - I_z^j (I_+^i - I_-^i)] \right], \end{aligned} \quad (56bis)$$

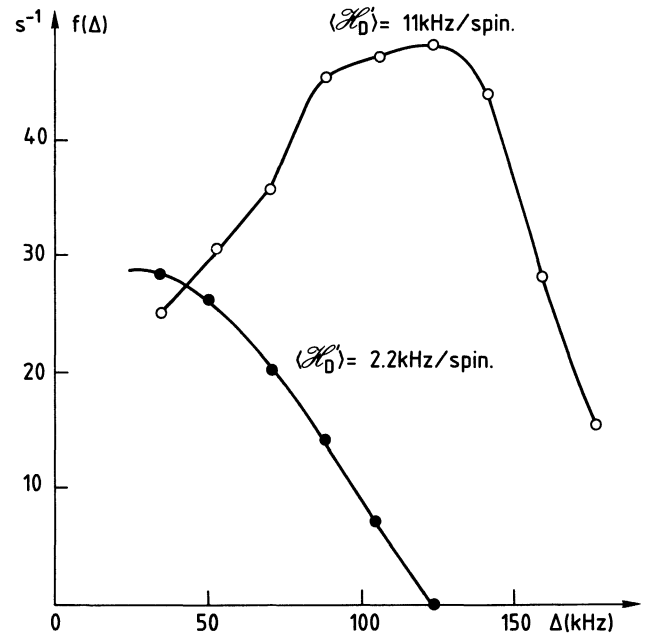


Fig. 15. — Weighted mixing rate $f(\Delta)/p_{eq}$ deduced from the results of figure 14 for 2 values of $\langle \mathcal{H}'_D \rangle$.

with

$$\begin{aligned} c_{ij} &= \cos(\theta_i - \theta_j), \quad s_{ij} = \sin(\theta_i - \theta_j), \\ I_+^i &= I_x^i + iI_y^i \quad \text{and} \quad I_-^i = I_x^i - iI_y^i. \end{aligned}$$

Using a standard R.P.A. approach we look for operators α and α^\dagger which are linear combinations of the I_+ 's and I_- 's and which obey :

$$[\mathcal{H}'_d, \alpha^\dagger] = \omega \alpha^\dagger \quad \text{and} \quad [\alpha, \alpha^\dagger] = 1.$$

The operators α and α^\dagger are determined in appendix. For each wave vector, we find two excitations which we call β and γ . The associated operators $\beta(\mathbf{k})$, $\beta^\dagger(\mathbf{k})$, $\gamma(\mathbf{k})$, $\gamma^\dagger(\mathbf{k})$ are linear combinations of the Fourier transforms $I_+^a(\mathbf{k})$ and $I_-^a(\mathbf{k})$ of I_+ and I_- ($a = 1, 2$). The definition of $I_+^a(\mathbf{k})$ and $I_-^a(\mathbf{k})$ is the same as that of $p_+^a(\mathbf{k})$ and $p_-^a(\mathbf{k})$ in section 3.2. The operators β and β^\dagger are symmetric with respect to interchange of indices 1 and 2, whereas γ and γ^\dagger are antisymmetric. The excitation frequency is given by :

$$\omega_\beta^2(\mathbf{k}) = \frac{p_\perp^2}{4} D(\mathbf{k}_0) (D(\mathbf{k}_0) - A(\mathbf{k}) \mp R_e B(\mathbf{k})). \quad (57)$$

Figure 16 shows the density of modes calculated according to (57) for $p_\perp = 60\%$. It is seen that the excitation energies all lie close to the Weiss field frequency $\omega_i = \gamma_\perp H_i$.

3.5.2. Coupling of the P spins to the Tm spin waves. — The operator V (Eq. (52)) responsible for the Tm-P transitions can be expressed in terms of the spin wave creation and annihilation operators. In section 3.4.2, the simplified form of the Weiss field Hamiltonian

allowed us to decouple the interactions of one P spin with its various Tm neighbours. Here however the correlation effects between Tm neighbours are explicitly taken into account by the R.P.A. approximation and V must now be understood as the sum of (52) taken over all Tm spins. From (52) and (56) we find :

$$V = \sin \theta S_X^\nu \sum_i B_{iv} I_X^i$$

$$= \sin \theta S_X^\nu \sum_k [B^{(1)}(\mathbf{k}) I^{(1)}(\mathbf{k}) + B^{(2)}(\mathbf{k}) I_X^{(2)}(\mathbf{k})]$$

where $B^{(1)}(\mathbf{k})$ and $B^{(2)}(\mathbf{k})$ are the Fourier transforms of the Tm-P interaction B_{iv} for Tm spins 1 and 2 respectively. By use of (A.2) and (A.3) V can be written as a linear combination of $\beta, \beta^\dagger, \gamma$ and γ^\dagger :

$$V = \sin \theta S_X^\nu \times$$

$$\times \sum_k [b(\beta^+(\mathbf{k}) + \beta(-\mathbf{k})) + c(\gamma^+(\mathbf{k}) + \gamma(-\mathbf{k}))],$$

with

$$b = \frac{1}{\sqrt{N}} \sqrt{\frac{p_\perp}{8}} (B^{(1)}(\mathbf{k}) + B^{(2)}(\mathbf{k})) \times$$

$$\times (\cosh \theta_\beta(\mathbf{k}) - \sinh \theta_\beta(\mathbf{k}))$$

$$\text{and } c = \frac{1}{\sqrt{N}} \sqrt{\frac{p_\perp}{8}} \times$$

$$\times (B^{(1)}(\mathbf{k}) - B^{(2)}(\mathbf{k})) (\cosh \theta_\gamma(\mathbf{k}) - \sinh \theta_\gamma(\mathbf{k})).$$

The effect of V is to induce transitions of the P spin between states $S_z = 1/2$ and $S_z = -1/2$ with the simultaneous creation or destruction of spin waves of frequency $\omega(\mathbf{k})$. By summing the matrix elements of V over all possible spin wave states one can write a rate equation for the populations $p_{1/2}$ and $p_{-1/2}$ of the two P states :

$$\frac{dp_{1/2}}{dt} = \frac{-dp_{-1/2}}{dt} =$$

$$= -\sin^2 \theta \frac{p_\perp}{1-r} (\mu_\beta + \mu_\gamma) (rp_{1/2} - p_{-1/2}) \quad (58)$$

where :

$$r = \exp - (\hbar \Delta / kT)$$

and :

$$\mu_\beta = \frac{\pi}{16N} \sum_k |B^{(1)}(\mathbf{k}) + B^{(2)}(\mathbf{k})|^2 \times$$

$$\times [\cosh \theta^\beta(\mathbf{k}) - \sinh \theta^\beta(\mathbf{k})]^2 \delta(\Delta - \omega_\beta(\mathbf{k}))$$

$$\mu_\gamma = \frac{\pi}{16N} \sum_k |B^{(1)}(\mathbf{k}) - B^{(2)}(\mathbf{k})|^2 \times$$

$$\times [\cosh \theta^\gamma(\mathbf{k}) - \sinh \theta^\gamma(\mathbf{k})]^2 \delta(\Delta - \omega_\gamma(\mathbf{k})).$$

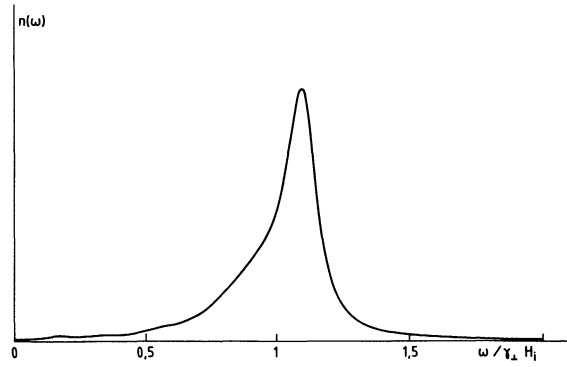


Fig. 16. — Density $n(\omega)$ of spin wave modes (arbitrary units) as a function of the reduced frequency $\omega/(\gamma_\perp H_i)$ according to the R.P.A. model.

When the P polarization is zero, $p_{1/2} = p_{-1/2} = 1/2$, and p grows as :

$$\frac{dp}{dt} = \frac{dp_{1/2}}{dt} - \frac{dp_{-1/2}}{dt} = \sin^2 \theta p_\perp (\mu_\beta + \mu_\gamma),$$

whence we deduce :

$$g(\Delta) = \frac{1}{\sin^2 \theta} \frac{dp}{dt} = p_\perp (\mu_\beta + \mu_\gamma). \quad (59)$$

From (58) it is easily shown that the growth of p is exponential toward p_{eq} at a rate $W = \sin^2 \theta \frac{g(\Delta)}{p_{eq}}$, with p_{eq} given by (54).

3.5.3 Comparison with the experiment. — Figure 17 shows the shape of $g(\Delta)$ predicted by (59) for $p_\perp = 61\%$. It is much narrower than the experimental curve. The narrowness of the theoretical peak is a consequence of the very small dispersion of the spin wave frequencies around the Weiss field frequency. Although formula (59) is unable to predict correctly the experimental width of $g(\Delta)$, it gives a fairly good value for the area

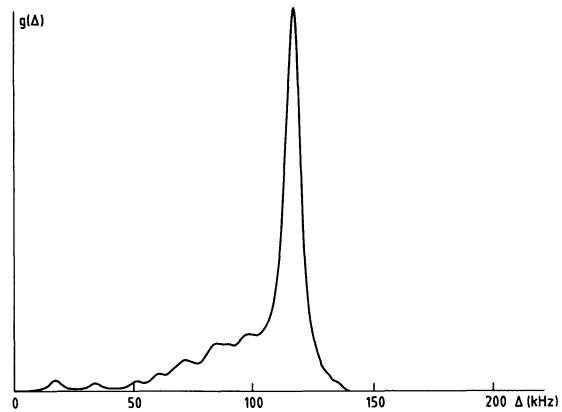


Fig. 17. — Theoretical value of the weighted mixing rate $g(\Delta)$ (arbitrary units) for $p_\perp = 61\%$ according to the R.P.A. model.

$\int g(\Delta) d\Delta$: the experimental and the theoretical values are respectively 15.7×10^6 and $14.1 \times 10^6 \text{ s}^{-2}$. We may thus conclude that the spin wave theory accounts correctly for the Tm-P coupling strength but that there is some additional broadening mechanism.

We have examined two possible mechanisms for the observed broadening of $g(\Delta)$:

Firstly, the collisions of spin waves with impurities or with other spin waves ; our estimate of this effect indicates that, although it is not completely negligible it cannot account for the observed effect.

Secondly, an inhomogeneity of the transverse polarization p_{\perp} . For a number of reasons the Tm polarization obtained by D.N.P. may be inhomogeneous : for instance the sample temperature may be inhomogeneous under H. F. irradiation, or the inhomogeneously broadened Yb-E.P.R. line may induce some « unobservable » inhomogeneity of the nuclear polarization (cf. Sect. 2.4). From the Tm N.M.R. we know only that the average Tm polarization after D.N.P. is 60 % and this leaves room for a significant r.m.s. inhomogeneity. Only by polarizing the Tm spins to almost 100 % could we be sure that the polarization is homogeneous. Inhomogeneity in the polarization will lead after demagnetization to a spread Δp_{\perp} of p_{\perp} around its average value \bar{p}_{\perp} and, since the peak of $g(\Delta)$ is roughly at $q\bar{p}_{\perp}$, the broadening due to the dispersion of p_{\perp} will be of the order of $q\Delta p_{\perp}$. We have taken this effect into account by convoluting $g(\Delta)$ with a Gaussian profile of r.m.s. deviation Δp_{\perp} . Figure 18 shows the result for various values of \bar{p}_{\perp} and for a plausible value of Δp_{\perp} which is assumed to be independent of \bar{p}_{\perp} and equal to 0.15. From a comparison of these theoretical curves with the experimental ones of figure 14, we deduce for $\langle \mathcal{H}'_d \rangle = -11 \text{ kHz/spin}$ a value of $\bar{p}_{\perp} = 67\%$. This value is more reasonable than the 73 % found by assuming a homogeneous initial polarization,

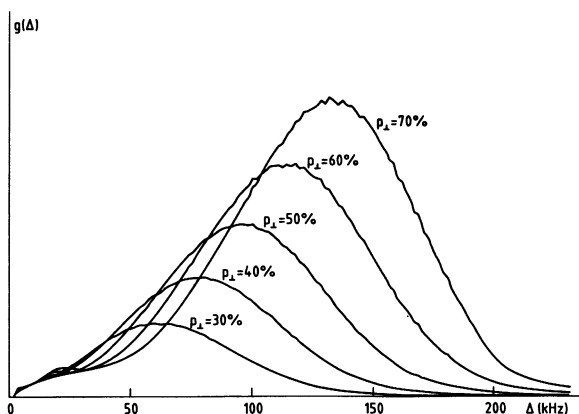


Fig. 18. — Weighted mixing rate $g(\Delta)$ (arbitrary units) according to the RPA model assuming a r.m.s. dispersion of p_{\perp} equal to 0.15.

but is still substantially higher than the starting polarization. This is probably due to the rather approximate fashion in which the inhomogeneity was taken into account. For smaller values of \bar{p}_{\perp} , the R.P.A. approximation becomes questionable and we did not attempt to extend the quantitative analysis to this regime.

4. Conclusions.

The advantages of « enhanced » nuclei as compared to « normal » nuclei, for the study of nuclear magnetic ordering « in the laboratory frame » are essentially 1) a high critical temperature and 2) a short relaxation time. On the contrary, for the studies of ordering « in the rotating frame », we were not at all attracted by a short relaxation time, nor particularly by a high critical temperature, but rather by the strong anisotropy of the material, which favours the transverse rotating ordered phases. The theoretical situation to this respect is simpler than in CaF_2 , where the transverse phase is quasi-degenerate with a longitudinal one.

The price to pay for this theoretical simplicity is a high sensitivity of the results to orientation, which deteriorates the precision of the measurements and makes it necessary to control carefully the orientation of the magnetic field with respect to the crystalline axes.

There is no doubt that we successfully produced the transverse ordered phase, the clearest proof of it being the Tm-P double resonance experiment. However, comparison of the experimental results with the existing theories is not completely satisfactory : on the one hand, the long-range dipolar energy deduced from the total dipolar energy measurements indicates a transverse polarization of order 40 % ; on the other hand, analysis of the Tm-N.M.R. resonance and of the Tm-P double resonance are more consistent with a higher value (60-70 %). As a matter of fact, the interpretation of the results is certainly hampered by the experimental drawbacks mentioned above.

Whatsoever, it should be remarked that this experiment is the first one of nuclear magnetic ordering in the rotating frame with enhanced nuclei. This contrasts with the number of results already reported of ordering in the laboratory frame with several Van Vleck compounds. Unfortunately, TmPO_4 does not belong (so far) to the list, probably because of its small enhancement : there still remains to find a compound where both types of ordering could be produced, allowing some interesting comparisons.

Acknowledgments.

The authors wish to thank gratefully Dr. M. Goldman for his interest in this work and for numerous fruitful discussions.

Appendix.

DETERMINATION OF THE SPIN WAVES. — The Hamiltonian (56bis) is first written in Fourier space, and its commutators with $I_+^a(\mathbf{k})$ and $I_-^a(\mathbf{k})$ ($a = 1, 2$) are calculated. The commutators which are bilinear combinations of the $I^a(\mathbf{k})$'s are simplified according to the standard R.P.A. rules. For instance, a term $I_Z^a(\mathbf{k}) I_+^a(\mathbf{k}')$ is replaced by :

$$\begin{aligned} \langle I_Z^a(\mathbf{k}) \rangle \langle I_+^a(\mathbf{k}') \rangle + \langle I_Z^a(\mathbf{k}) \rangle (I_+^a(\mathbf{k}') - \langle I_+^a(\mathbf{k}') \rangle) + (I_Z^a(\mathbf{k}) - \langle I_Z^a(\mathbf{k}) \rangle) \langle I_+^a(\mathbf{k}') \rangle = \\ = \sqrt{N} \frac{P_\perp}{2} I_+(\mathbf{k}') \delta(\mathbf{k}) \delta_{a,a'} \end{aligned}$$

since
$$\langle I_Z^a(\mathbf{k}) \rangle = \sqrt{N} \frac{P_\perp}{2} \delta(\mathbf{k}),$$

and
$$\langle I_+^a(\mathbf{k}) \rangle = 0.$$

A term $I_Z^a(\mathbf{k}) I_Z^a(\mathbf{k}')$ is replaced by $N \frac{P_\perp^2}{4} \delta(\mathbf{k}) \delta(\mathbf{k}') \delta_{a,a'}$, since the deviations of I_Z from equilibrium are of higher order than those of I_+ and I_- in the R.P.A. approximation.

Under these approximations, the four commutators are given by the matrix equations :

$$\begin{bmatrix} \mathcal{H}'_{\mathbf{d}^-}, I_-^{(1)}(\mathbf{k}) \\ \mathcal{H}'_{\mathbf{d}^+}, I_+^{(1)}(\mathbf{k}) \\ \mathcal{H}'_{\mathbf{d}^-}, I_-^{(2)}(\mathbf{k}) \\ \mathcal{H}'_{\mathbf{d}^+}, I_+^{(2)}(\mathbf{k}) \end{bmatrix} = \begin{bmatrix} E & F & G & H \\ -F & -E & -H & -G \\ G & H & E & F \\ -H & -G & -F & -E \end{bmatrix} \begin{bmatrix} I_-^{(1)}(\mathbf{k}) \\ I_+^{(1)}(\mathbf{k}) \\ I_-^{(2)}(\mathbf{k}) \\ I_+^{(2)}(\mathbf{k}) \end{bmatrix} = M \begin{bmatrix} I_-^{(1)}(\mathbf{k}) \\ I_+^{(1)}(\mathbf{k}) \\ I_-^{(2)}(\mathbf{k}) \\ I_+^{(2)}(\mathbf{k}) \end{bmatrix}$$

with :

$$\begin{aligned} E &= \frac{P_\perp}{2} \left[A(\mathbf{k}_0) + R_e B(\mathbf{k}_0) - \frac{1}{4} (A(\mathbf{k} + \mathbf{k}_0) + A(\mathbf{k} - \mathbf{k}_0)) \right] \\ F &= \frac{P_\perp}{8} [A(\mathbf{k} + \mathbf{k}_0) + A(\mathbf{k} - \mathbf{k}_0)] \\ G &= -H = -\frac{P_\perp}{8} R_e [B(\mathbf{k} - \mathbf{k}_0) + B(\mathbf{k} + \mathbf{k}_0)]. \end{aligned}$$

The creation and annihilation operators are eigenvectors of M and, since M is invariant under the exchange of index 1 and 2, they are either of the symmetric or antisymmetric type. We call them β and β^\dagger in the first case, γ and γ^\dagger in the second case. They obey the commutation rules :

$$[\beta(\mathbf{k}), \beta^\dagger(\mathbf{k})] = [\gamma(\mathbf{k}), \gamma^\dagger(\mathbf{k})] = 1, \quad (\text{A. 1})$$

and are of the form :

$$\begin{aligned} \beta^\dagger(\mathbf{k}) &= \mu_\beta(\mathbf{k}) I_-^s(\mathbf{k}) + v_\beta(\mathbf{k}) I_+^s(\mathbf{k}) \\ \gamma^\dagger(\mathbf{k}) &= \mu_\gamma(\mathbf{k}) I_-^A(\mathbf{k}) + v_\gamma(\mathbf{k}) I_+^A(\mathbf{k}) \end{aligned}$$

with

$$\begin{aligned} I_\pm^s(\mathbf{k}) &= I_\pm^{(1)}(\mathbf{k}) + I_\pm^{(2)}(\mathbf{k}) \\ I_\pm^A(\mathbf{k}) &= I_\pm^{(1)}(\mathbf{k}) - I_\pm^{(2)}(\mathbf{k}). \end{aligned}$$

(A. 1) together with :

$$[I_+^s(\mathbf{k}), I_-^s(\mathbf{k})] = [I_+^A(\mathbf{k}), I_-^A(\mathbf{k})] = 2 p_\perp$$

yields :

$$u_\beta^2(\mathbf{k}) - v_\beta^2(\mathbf{k}) = \frac{1}{2 p_\perp}.$$

We can take :

$$u_{\gamma}(\mathbf{k}) = \frac{1}{\sqrt{2 p_1}} \cosh \theta_{\gamma}(\mathbf{k})$$

$$v_{\gamma}(\mathbf{k}) = \frac{1}{\sqrt{2 p_1}} \sinh \theta_{\gamma}(\mathbf{k}).$$

With these notations one finds for the eigenfrequencies :

$$\omega_{\gamma}^2(\mathbf{k}) = E^2(\mathbf{k}) - F^2(\mathbf{k}) \mp 2 G(\mathbf{k}) (E(\mathbf{k}) + F(\mathbf{k}))$$

and for $\theta_{\gamma}(\mathbf{k})$:

$$\tanh \theta_{\gamma}(\mathbf{k}) = \left[1 - \frac{E(\mathbf{k}) + F(\mathbf{k})}{\omega_{\gamma}(\mathbf{k})} \right] / \left[1 + \frac{E(\mathbf{k}) + F(\mathbf{k})}{\omega_{\gamma}(\mathbf{k})} \right].$$

We note that $\tan \theta_{\gamma}(\mathbf{k})$ is only a function of $\omega_{\gamma}(\mathbf{k})$.

In the case of TmPO_4 , $B(\mathbf{k}_0)$ is real ; moreover k_0 is vanishing small so that for most of the Brillouin zone one has : $k \gg k_0$. We can then write :

$$A(\mathbf{k}_0) + R_e B(\mathbf{k}_0) = A(\mathbf{k}_0) + B(\mathbf{k}_0) = D(\mathbf{k}_0)$$

and

$$A(\mathbf{k} + \mathbf{k}_0) + A(\mathbf{k} - \mathbf{k}_0) \approx 2 A(\mathbf{k})$$

whence :

$$\omega_{\gamma}^2(\mathbf{k}) \approx \frac{p_1^2}{4} D(\mathbf{k}_0) (D(\mathbf{k}_0) - A(\mathbf{k}) \pm R_e B(\mathbf{k})).$$

References

- [1] ^3He : OSHEROFF, D. D., CROSS, M. C. and FISHER, D. S., *Phys. Rev. Lett.* **44** (1980) 798.
- [2] CaF_2 : GOLDMAN, M., CHAPPELLIER, M., VU HOANG CHAN and ABRAGAM, A., *Phys. Rev.* **B 10** (1974) 226.
- [3] CaF_2 : URBINA, C., JACQUINOT, J. F. and GOLDMAN, M., *Phys. Rev. Lett.* **48** (1982) 206.
- [4] LiF : COX, S. F. J., BOUFFARD, V. and GOLDMAN, M., *J. Phys. C Solid State* **8** (1975) 3664.
- [5] LiH : ROINEL, Y., BACCHELLA, G. L., AVENEL, O., BOUFFARD, V., PINOT, M., ROUBEAU, P., MERIEL, P. and GOLDMAN, M., *J. Physique Lett.* **41** (1980) L-123.
- [6] Ca(OH)_2 : WENCKEBACH, W. Th., *Physica* **B 127** (1984) 296.
- [7] GOLDMAN, M., *Phys. Rep.* **32** (1977) 1.
- [8] For the most recent review of nuclear magnetic ordering in diamagnetic crystals see ABRAGAM, A. and GOLDMAN, M., *Nuclear magnetism : order and disorder* (Clarendon Press, Oxford) 1982, chapter 8.
- [9] HUIKU, M. T., JYRKIÖ, T. A., KYYNÄRÄINEN, J. M., OJA, A. S. and LOUNASMAA, O. V., *Phys. Rev. Lett.* **53** (1984) 1692 and references therein.
- [10] HoVO_4 : SUZUKI, H., NAURBUDRIPAD, N., BLEANEY, B., ALLSOP, A. L., BOWDEN, G. J., CAMPBELL, I. A. and STONE, N. J., *J. Physique Colloq.* **39** (1978) C6-800.
- [11] PrCu_6 : BABCOCK, J., KIELY, J., MANLEY, J. and WEYHMANN, W., *Phys. Rev. Lett.* **43**, 380 (1979).
- [12] PrNi_5 : KUBOTA, M., FOLLE, H. R., BUCHAL, Ch., MUELLER, R. M. and POBELL, F., *Phys. Rev. Lett.* **45** (1980) 1812.
- [13] $\text{CS}_2\text{NaHoCl}_6$: SUZUKI, H., MIYAMOTA, M., MASUDA, Y. and OHTSUKA, T., *J. Low. Temp. Phys.* **48** (1982) 297.
- [14] PrCu_5 : GENICON, J. L., THOLENCE, J. L. and TOURNIER, R., *J. Physique Colloq.* **39** (1978) C6-798.
- [15] ABRAGAM, A., BOUFFARD, V., FERMON, C., FOURNIER, G., GREGG, J., JACQUINOT, J. F. and ROINEL, Y., *C.R. Hebd. Séan. Acad. Sci.* **299** (1984) 509.
- [16] ABRAGAM, A. and BLEANEY, B., *Proc. R. Soc. London* **A 387** (1983) 221.
- [17] BLEANEY, B., PASMAN, J. H. T. and WELLS, M. R., *Proc. R. Soc. London* **A 387** (1983) 75.
- [18] ROINEL, Y., BOUFFARD, V., JACQUINOT, J. F., FERMON, C. and FOURNIER, G., *J. Physique* (to be published).

- [19] SCOTT, P. L., STAPLETON, H. J. and WAINSTEIN, C., *Phys. Rev. A* **137** (1965) 71.
- [20] EGOROV, A. V., EREMIN, M. V., TAGIROV, M. S. and TEPLOV, M. A., *Sov. Phys. JETP* **50** (1979) 1145.
- [21] GOLDMAN, M., COX, S. F. J. and BOUFFARD, V., *J. Phys. C Solid State* **7** (1974) 2940.
- [22] COX, S. F. J., BOUFFARD, V. and GOLDMAN, M., *J. Phys. Lett.* **6** (1973) 100.
- [23] Same as Ref. [7], chapter 6.
- [24] ABRAHAM, M. M., BOATNER, L. A., RAMEY, J. O. and RAPPAZ, M., *J. Chem. Phys.* **78** (1983) 3.
- [25] BLEANEY, B., Private comm.
- [26] ROINEL, Y., BOUFFARD, V. and ROUBEAU, P., *J. Physique* **39** (1978) 1000.
- [27] ROINEL, Y. et BOUFFARD, V., *J. Physique* **38** (1977) 817.
- [28] URBINA, C., Thesis, Faculté des Sciences d'Orsay n° 2513 (1981).
- [29] URBINA, C., JACQUINOT, J. F. and GOLDMAN, M.; GOLDMAN, M., JACQUINOT, J. F. and URBINA, C., *J. Phys. C* **19** (1986) to be published.
- [30] GOLDMAN, M., *Spin Temperature and Nuclear Magnetic Resonance in Solids* (Clarendon Press, Oxford) 1970.
- [31] GOLDMAN, M. and FERMON, C., *J. Magn. Res.* **65** (1985) to be published.
- [32] COHEN, M. H. and KEFFER, F., *Phys. Rev.* **99** (1955) 1128.
- [33] GOLDMAN, M., *J. Magn. Res.* **17** (1975) 393.
- [34] HARTMANN, S. R. and HAHN, E. L., *Phys. Rev.* **128** (1962) 2042.
-